JOURNAL OF GEOPHYSICAL RESEARCH, VOL. 106, NO. D21, PAGES 27,673–27,699, NOVEMBER 16, 2001

Nitrogen oxides and ozone in the tropopause region of the Northern Hemisphere: Measurements from commercial aircraft in 1995/1996 and 1997

Dominik Brunner, Johannes Staehelin, Dominique Jeker, and Heini Wernli
Institute for Atmospheric and Climate Science, Swiss Federal Institute of Technology, Zurich, Switzerland

Ulrich Schumann
Institut für Physik der Atmosphäre, Deutsches Zentrum für Luft- und Raumfahrt, Oberpfaffenhofen, Germany

Abstract. Measurements of nitrogen oxides (NO and NO_2) and ozone (O_3) were performed from a Swissair B-747 passenger aircraft in two extended time periods (May 1995 to May 1996, August to November 1997) in the framework of the Swiss NOXAR and the European POLINAT 2 project. The measurements were obtained on a total of 623 flights between Europe and destinations in the United States and the Far East. NO_2 measnrements were obtained only after December 1995 and were less precise than the NO measurements. Therefore daytime NO_2 values were derived from measured NO and O_3 concentrations assuming photostationary equilibrium. The completed NO_x data set (measured NO, measured NO_2 during night, and calculated NO_2 during day) includes a complete annual cycle and is the most extensive and representative data set currently available for the upper troposphere (UT) and the lower stratosphere (LS) covering a significant proportion of the northern hemisphere between 15°N and 65°N. NO_x concentrations in midlatitudes (30°-60°N) showed a marked seasonal variation both in the UT and the LS with a maximum in summer (median/mean values of 159/264 pptv in UT, 199/237 pptv in LS) and a minimum in winter (51/99 pptv in UT, 67/91 pptv in LS). Mean NO_x concentrations were generally much higher than the respective median values, in particular in the UT, which reflects the important contribution from comparatively few very high concentrations observed in large-scale convection/lightning and small-scale aircraft plumes. Seasonal mean NO_x concentrations in the UT were up to 3-4 times higher over continental regions than over the North Atlantic during summer. Lightning production of NO and convective vertical transport from the polluted boundary layer thns appear to have dominated the upper tropospheric NO_x budget over these continental regions, particularly during summer. Ozone concentrations at aircraft cruising levels typically varied by an order of magnitude due to the strong vertical gradient in the LS. Seasonal mean values were dominated by large-scale dynamical processes controlling the altitude of the tropopause and the O_3 abundance in the LS. O_3 in the UT in midlatitndes showed a broad maximum between Jnne and August, typical of observations in the free troposphere.

1. Introduction

Nitrogen oxides (NO_x) play a key role in the formation of tropospheric ozone (O_3) [e.g., *Fishman and Crutzen*, 1978; *Crutzen*, 1988]. High O_3 concentrations in the atmospheric boundary layer (ABL) may have toxic effects on humans [*Lippmann*, 1991] and vegetation [*Prinz*, 1988]. O_3 is also a strong greenhouse gas, which reaches maximal radiative forcing near the cold tropopause [*Lacis et al.*, 1990; *Chalita et al.*, 1996]. The various chemical and dynamical processes affecting O_3 concentrations in the upper troposphere (UT) have therefore received increasing attention during recent years [*Intergovernmental Panel on Climate Change*, 1995].

One concern is a possible future increase in upper tropospheric NO_x concentrations due to emissions from the rapidly growing air traffic or due to the upward transport of pollutants released at the snrface. A NO_x molecule deposited in the UT may produce several times

Paper number 2001JD900239.
0148-0227/01/2001JD900239$09.00

more O_3 molecules than in the polluted ABL, because the catalytic production cycles are more efficient at low NO_x concentrations, and because the lifetime of NO_x rapidly increases with altitude [*Liu et al.*, 1987; *Jaeglé et al.*, 1998]. It is therefore important to know the fate of surface emissions, in particular to know what fraction is exported to the free troposphere [*Hov and Flatoy*, 1997; *Jacob et al.*, 1993]. As a result of the longer lifetime and higher wind speeds, NO_x and many other trace species may be transported over large distances in the UT, thus potentially affecting photochemistry and O_3 concentrations far away from the source regions. Pollution transport in the free troposphere between North America and Europe has been observed for instance by *Arnold et al.* [1997] and *Stohl and Trickl* [1999].

Several recent studies investigated the impact of aircraft NO_x emissions upon ozone and global warming [*NASA*, 1997; *Brasseur et al.*, 1998; *Thompson et al.*, 2000; *Schumann et al.*, 2000]. The common approach to estimate the contributions from various sources is to use a chemistry-transport-model (CTM) [*IPCC*, 1999]. The models indicate that aircraft emissions contribute most strongly to background concentrations at cruising altitudes (9-12 km) in northern midlatitudes (30°-60°N). In this region, aircraft emissions account for approximately 50-100 pptv of NO_x and for a maximum increase in O_3 of about 3-12 ppbv (3-9%) during summer.

In addition to aircraft emissions, convective upward transport from the surface, lightning activity, downward mixing from the stratosphere, and chemical recycling from reservoir species produced elsewhere in the atmosphere, make up relevant contributions to the budget of upper tropospheric NO_x [*Lamarque et al.*, 1996; *Dameris et al.*, 1998]. This mixture of sources, uncertainties in their strenghts (in particular of lightning), their link to complex transport processes such as convection and stratosphere-troposphere exchange, combined with the short lifetime of a few days, makes upper tropospheric NO_x concentrations particularly difficult to simulate with a model. Not surprisingly, recent intercomparisons of several state-of-the-art CTMs have revealed substantial differences between the calculated NO_x distributions [*Brasseur et al.*, 1998; *IPCC*, 1999].

Model results therefore need to be validated against measurements, but the availability of insitu observations has been very limited so far [*Emmons et al.*, 1997; *Bradshaw et al.*, 2000; *Thakur et al.*, 1999]. The use of commercial airliners as a platform to provide comprehensive measurements of a few key trace species in the tropopause region was already demonstrated in the late 1960s and 1970s [*Seiler and Junge*, 1970; *Fabian and Pruchniewicz*, 1977; *Nastrom*, 1979]. More recent examples of this approach are the European Measurement of Ozone on Airbus In-Service Aircraft (MOZAIC) [*Marenco et al.*, 1998] and Civil Aircraft for Remote Sensing and In-Situ Measurements Based on the Instrumentation Container Concept (CARIBIC) [*Brenninkmeijer et al.*, 1999] programs as well as the Japanese JAL program [*Matsueda and Inoue*, 1996]. Until today, none of these programs has provided measurements of nitrogen oxides. Measurements of NO_y from an Airbus have started very recently within the MOZAIC-III project. Also within CARIBIC it is planned to implement an instrument for the measurement of nitrogen oxides.

In this paper we present the results of extensive measurements of NO, NO_2, and O_3 accomplished in the framework of the Swiss Nitrogen Oxides and Ozone along Air Routes (NOXAR) and the second European Pollution from Aircraft Emissions in the North Atlantic Flight Corridor (POLINAT 2) project. The measurements were obtained from a commercial airliner (B-747-357 Combi operated by Swissair) from May 1995 until May 1996 (NOXAR) and from August to November 1997 (POLINAT 2). Previously, we reported on observations of frequent large-scale nitrogen oxide plumes, which typically extended several 100 km along the flight track and showed NO_x enhancements of 0.5-5 ppbv above background [*Brunner et al.*, 1998]. These plumes were associated with increased upper tropospheric O_3 concentrations, particularly during summer. *Jeker et al.* [2000] extended the analysis of such plumes in several case studies during the coordinated SONEX/ POLINAT 2 campaign in 1997. They demonstrated the close link of such plumes to convective activity and lightning, applying a new method for the tracing of lightning events along calculated backward trajectories. A comparison of upper tropospheric NO_x concentrations simulated by two general circulation models with observations from NOXAR was recently shown by *Grewe et al.* [2001]. *Emmons et al.* [2000] presented a comparison of the B-747 measurements with observations from a large number of scientific aircraft campaigns, which demonstrated the significant increase in data coverage achieved by the NOXAR project.

Here we present a more complete climatology of the observations. The data set comprises 70% more NO_x data than previously used by *Brunner et al.* [1998] by including the POLINAT 2 data as well as nighttime measurements of NO_2. The focus of this paper is placed on the characterization of the geographical and seasonal distributions of the measured tracers. Section 2 presents the instrumentation and a method to discriminate between samples obtained in the UT and the LS. Section 3 gives an overview of the project and the data coverage. In section 4 we present the seasonal and spatial variability of the observed NO_x and O_3 concentrations, separately for the UT and the LS. Specific attention is paid here to the characterization of the remarkably high variability of NO_x concentrations at cruising altitudes. A comparison between the observations in autumn obtained in two different years

(1995 and 1997) is presented in section 4.3. Finally, tropopause-scaled vertical profiles of NO_x and O_3 are shown in sections 4.4 and 4.5.

2. Instrumentation and Methods

2.1. Overview of the Design

The measurement system was permanently installed in the rear of a large cargo compartment on the main deck of a Swissair B-747 airliner. The instrumentation package consisted of commercial analyzers for the measurement of NO, NO_2, and O_3, a calibration and zero air supply system, and auxiliary equipment including pumps and electronic devices. A computer controlled the fully automatic operation of the system during flights and recorded the chemical measurements and controlling parameters as well as meteorological and positional data from the flight data recorder. Data from the aircraft were recorded every second and data from the chemical sensors every three seconds. In the present study, however, only 2-min averaged data are used. Start-ups after takeoff and shut downs before landing were triggered by the position of the aircraft's flaps and other flight information, and various calibrations were initiated at regular time intervals. A more detailed description of the instrumentation, its performance, and several aspects of its delicate implementation in a commercial airliner were presented by *Dias-Lalcaca et al.* [1998] and *Brunner* [1998]. Only the main characteristics of the system and a more detailed consideration of the treatment of the NO_2 measurements which had been excluded in the previous study of *Brunner et al.* [1998] is presented here.

Two standard chemiluminescence detectors (CLDs) produced by ECO Physics Inc., Switzerland, were used to measure NO. A photolytic converter upstream of the second analyzer converted NO_2 to NO with a high efficiency of approximately 65% at a residence time of only 2.5 s [*Dias-Lalcaca et al.*, 1998]. The concentration of NO_2 was then calculated from the difference in NO measured by the two analyzers and the efficiency of the converter.

Periodic calibrations allowed to determine (1) the instrumental background signals (every 20 minutes), (2) the sensitivities of the NO analyzers (typically twice per flight), and (3) the efficiency of the photolytic converter (also twice per flight). Ozone was monitored by a modified Environics S-300 analyzer based on the UV-absorption technique.

2.2. Data Quality

2.2.1. General performance. Detection limits (1 σ) of 23, 45 and 500 pptv and accuracies of 8%, 11%, and 6% were achieved for NO, NO_2, and O_3, respectively, for a 2-min integration time [*Dias-Lalcaca et al.*, 1998]. While daytime NO concentrations were usually well above the detection limit, the same is not true for NO_2. The largest source of uncertainty for the 2-min averaged data was identified to be the precision of the zero-point calibrations, which were started at regular 20-min time intervals during each flight [*Brunner*, 1998]. During these calibrations the instruments were supplied with purified (virtually NO_x free) air to determine the instrumental background signals. These signals were then interpolated linearly between calibrations to the times of the measurements. Therefore an error in the zero-point calibration affected all samples in the preceding and following 20-min time intervals. In particular, the measured NO_2 concentrations, which may suffer from calibration errors in both instruments, could accidentally be seriously in error over a time period of at least 20 min. Since these errors were random in nature, averaging over large numbers of samples as done in the present study is expected to average out most of these inaccuracies.

In the absence of sunlight, NO is rapidly titrated by O_3 and we expected near-zero concentrations at night. However, nighttime measurements usually showed slightly negative concentrations. We believe that this is an instrumental artifact rather than a possible interference with other trace species, since the offset varied with operation time and operatiou mode (slightly higher immediately after a calibration), but no correlation was found with O_3. If the offset was caused by interference with other tracers such as unsaturated hydrocarbons, PAN, HNO_4 or H_2O_2 [*Drummond et al.*, 1985; *Fontijn et al.*, 1970; *Bollinger*, 1982] these tracers would most likely have a pronounced gradient across the tropopause and hence we would expect a correlation with O_3. The offset was 7.6 pptv on average and exceeded 10 pptv only in 4 out of 12 months during 1995/1996. The largest offset of about 30 pptv was seen during 10 days in June when the NO instrument was temporarily replaced by an instrument of identical make but unfortunately of reduced performance. The June measurements are therefore of somewhat lower quality. An average offset depending on the time after start-up of the instruments was determined for each month separately and subtracted from the measured NO values. An estimate of the uncertainty introduced by this offset-correction is included in the overall uncertainties stated above [*Dias-Lalcaca et al.*, 1998].

The instrumental artifact of the second analyzer could only be determined on comparatively few flights when the lamp of the photolytic converter was turned off and the second analyzer therefore also measured NO. Different from the other instrument, no significant offset was found in the nighttime measurements and no correction was therefore applied to the concentrations measured by this device.

Measurements during ascent and descent at the be-

ginning and end of a flight suffered from a number of problems. A strong drift in the instrumental background signals declined the quality of the NO and NO_2 measurements during these phases. There are at least three known sources to this problem: (1) decay of photomultiplier darkcount after the instrument is turned on (note that safety regulations required that the instruments were turned off during takeoff), (2) change of spurious signal from cosmic rays which is depending on altitude [*Ridley et al.*, 1987], and (3) change of the background signal due to changes in humidity [*Schiff et al.*, 1979; *Carroll et al.*, 1985; *Drummond et al.*, 1985]. Additionally, the pressure regulation system failed to maintain the required constant pressure at the inlet of the CLDs below 6000 m altitude. The quality of the O_3 measurement during ascent and descent was affected by a humidity interference at high water vapor concentrations in the lower and middle troposphere [*Jeker et al.*, 2000]. Throughout this study, we therefore exclude the measurements obtained during ascent and descent and concentrate on quality-controlled observations obtained at cruising altitudes between 330 hPa and 200 hPa (about 8.5 to 11.6 km).

2.2.2. Modifications for POLINAT 2. Some modifications were made for the POLINAT 2 campaign in 1997 mainly to improve the performance of the instruments during ascent and descent. The modifications included (1) humidification of the O_3 supply to the CLDs, (2) tying NO calibration standard to DLR (Deutsches Zentrum für Luft- und Raumfahrt) standard, and (3) change of absorption tubes in ozone analyzer. The latter was necessary because during a test the glass tube used in 1995/1996 was broken and after evaluating several different tubes for their sensitivity to the water vapor interference it was decided to retrofit the original PTFE-coated tube. Furthermore, the NO instruments were now switched at 2 min time intervals during 30 s to prechamber mode [*Drummond et al.*, 1985], which allowed a better quantification of the drift of the instrumental background. This improved the measurements during ascent and descent while no improvement was achieved at cruising levels. Humidification of the O_3 supply as suggested by *Drummond et al.* [1985] slightly reduced the baseline drift of the CLDs, which further improved the measurements during ascent and descent. Tying the NO calibration standard (small 1 L cylinders were used on the airplane which were filled from the same 40 L cylinder (6 ppmv NO in N_2) during NOXAR and POLINAT 2) to DLR standard lead to a correction of the POLINAT 2 measurements by -5%. The POLINAT 2 data were therefore rescaled to the previous conditions, keeping in mind that according to this calibration the NOXAR measurements might be 5% too high, which is in the range of the stated accuracy of the NO_x measurements.

2.2.3. Measurement intercomparisons. A comparison between NOXAR and simultaneous O_3 measurements from an Airbus aircraft performed by the MOZAIC programme at cruising altitudes showed excellent agreement [*Dias-Lalcaca et al.*, 1998].

During POLINAT 2 an intercomparison flight was organized with the Falcon aircraft operated by DLR. Although the measurements agreed within the combined errors of the instruments, the results were not conclusive. The conditions for an intercomparison were unfavorable, due to crossing of many aged aircraft plumes by both the Falcon and the B-747 aircraft [*Jeker et al.*, 1999]. NO measurements from the DLR Falcon were also performed over the North Atlantic in June/July 1995 during the POLINAT 1 campaign [*Schumann*, 1996]. A planned intercomparison flight failed at that time but the mean and median concentrations measured from the Falcon aircraft on four flights between June 24 and June 29 agreed well with the B-747 observations obtained on four flights during the same time period and over the same sampling region [*Brunner*, 1998].

2.3. Measurement and Calculation of NO_2 and NO_x

The NO_2 measurements were seriously affected by a contamination problem between 5 May and 26 November 1995. Only NO_2 measurements obtained after that period are therefore used in this study. During daytime an approximate concentration NO_2* was derived from measured NO and O_3 concentrations in addition to measured NO_2 values, assuming a photostationary equilibrium:

$$[NO_2^*] = \frac{k_1[NO][O_3]}{J_{NO_2}}. \quad (1)$$

NO_2 was marked by a star in this equation in order to distinguish between calculated and measured values. Similarly, we define NO_x* as the sum of measured NO plus calculated NO_2*, thus $NO_x^* \equiv NO + NO_2^*$.

Under the conditions at the tropopause the equilibrium (1) is established within a few minutes. k_1 is the temperature-dependent rate coefficient for the reaction of $NO+O_3+M \rightarrow NO_2+O_3$ [*Atkinson et al.*, 1997]. Ambient temperatures were provided by the aircraft data acquisition system. NO_2 photolysis rates J_{NO_2} were taken from a lookup table generated with the System for Transfer of Atmospheric Radiation (STAR) model [*Ruggaber et al.*, 1994]. In order of importance the relevant parameters for the calculation of J_{NO_2} are the solar zenith angle, the ground albedo, the total aerosol optical depth, the aerosol single scattering albedo, the aerosol growth with relative humidity, and the NO_2 total content [*Ruggaber et al.*, 1994]. The lookup table lists J_{NO_2} values at different altitudes and solar zenith angles (0°-85°) for clear-sky conditions and climatological annual mean aerosol, NO_2 and O_3 columns, and average surface albedo. The same photochemical equilibrium (1) based on photolysis rates derived from

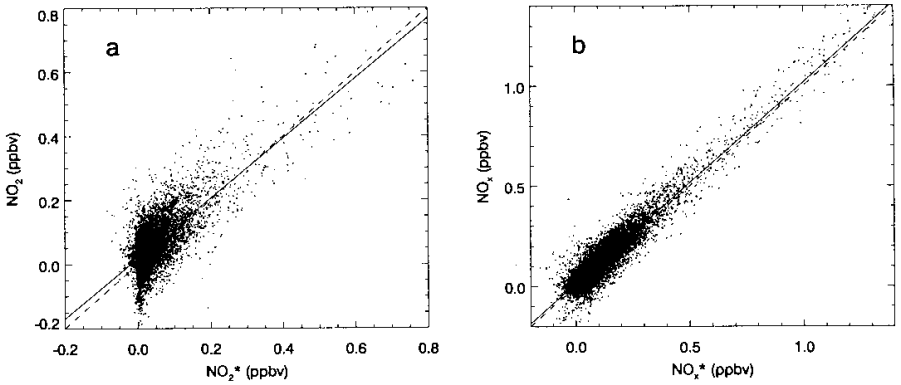

Figure 1. Scatterplots of (a) measured NO_2 versus computed NO_2* and (b) NO_x (=NO+NO_2) versus NO_x* (=NO+NO_2*). The dashed line is the 1:1 ratio, and the solid line is a linear fit through the points. Correlation coefficients are (a) r^2=0.56 and (b) r^2=0.95.

the model STAR has been previously used and tested against observations by *Schlager et al.* [1997].

Significant deviations from the equilibrium (1) can be expected in the presence of large concentrations of peroxy radicals and ClO and BrO [*Ridley et al.* 1992; *Davis et al.*, 1993; *Gao et al.*, 1997]. While the reaction of NO with these radicals decreases the ratio of NO:NO_2, the presence of clouds below the airplane increases it through the effect on J_{NO_2}. Since these factors could not be accounted for, equation (1) is only a first-order approximation. However, in the UT NO_2* made up only 17% of total NO_x* on average during daytime. *Crawford et al.* [1996, Figure 7b] have calculated similarly low ratios for PEM-West A data at altitudes between 9 and 12 km. Calculated NO_2:NO ratios in their study were in the range of about 0.1 to 0.4 (i.e., 0.09 to 0.29 for the ratio NO_2:NO_x). In the LS, NO_2* made up a larger fraction of 35% on average during daytime because of the higher O_3 concentrations.

Figure 1 shows the correlations between NO_2 and NO_2* and between NO_x and NO_x*. Linear regression of measured versus calculated NO_2 (Figure 1) yields

$$[NO_2] = 18 \text{ pptv} + 0.939[NO_2^*]. \quad (2)$$

This is a somewhat better agreement between measured and theoretical NO_2 concentrations than previously reported by *Dias-Lalcaca et al.* [1998] because the NO_2 data presented in that study were not yet corrected for the instrumental artifact of the NO instrument. However, the correlation (r^2=0.56) is still rather poor. The large scatter about the linear fit (1σ = 54 pptv) is a consequence of the low precision of the NO_2 measurement and of variations in J_{NO_2} not accounted for in the modeled values. The intercept of the linear fit is significantly different from zero, pointing toward an unresolved problem in the measurement. Potential candidates for causing the remaining offset are interferences from N_2O_5 and HNO_4 which may thermally decay in the sampling lines thereby forming additional NO_2. In the Teflon tubing the sample air is rapidly heated up to the ambient temperatures in the cargo compartment of 15°C to 20°C. Owing to the short residence time in the sampling lines and the active cooling of the PLC to about 6°C, gas phase thermal losses of the above species were estimated to be only of the order of 2%. Heterogeneous reactions on the walls of the tubing and the converter, however, may have increased the losses [*Carroll et al.*, 1990], yet to an unknown degree.

Because of the relatively small contribution of NO_2 to NO_x in the tropopause region, the correlation between NO_x and NO_x* is much better (Figure 1b):

$$[NO_x] = 15 \text{ pptv} + 1.003[NO_x^*]. \quad (3)$$

The large RMS error of 54 pptv is again mainly attributable to the low precision of the NO_2 measurement. The high correlation (r^2=0.95) and a slope close to unity however demonstrate that the assumption of a simple photostationary equilibrium is a good approximation at aircraft cruising altitudes. As discussed above, the nonzero offset of 15 pptv is possibly due to interferences with the thermally unstable molecules N_2O_5 and HNO_4. Owing to the low precision of the NO_2 measurement, potential interference problems, and the lack of NO_2 measurements before December 1995, we prefer calculated to measured NO_2 values in the following. Only on nighttime flights, when NO_x* can not be calculated and NO_2 concentrations are relatively high, measured NO_x values were used when available. These were corrected uniformly for the average offset of 15 pptv according to equation (3), although it is clear that the offset, if caused by interferences, is unlikely to have stayed constant for all measurements. The additional use of NO_2 measurements significantly increased the data coverage and filled several gaps over regions

which were always traversed at night, in particular at high latitudes during winter.

Between December 1995 and May 1996 when simultaneous data of NO_2 and NO_2* were available, mean daytime concentrations of NO_x (without correction for the offset) and NO_x* were 160 pptv and 145 pptv, respectively, a difference of only 11%. We therefore conclude that the uncertainty introduced by using theoretical NO_2* values adds to the uncertainty in total NO_x by not more than 11% on average. Occasionally however, in particular on flight legs in the LS, above clouds, or in air masses with high HO_2, BrO or ClO concentrations the error could be higher, yet unlikely exceeding the typical NO_2 fractions of 17% expected in the UT and 35% in the LS.

The uncertainty in the NO_x* data is now composed of the precision and accuracy of the NO measurement and the uncertainty in the calculated NO_2:NO_x ratio. Assuming a typical fraction of 25% of NO_2 (i.e., 75% is NO), the uncertainty of the 2-min averaged NO_x* data was estimated to about ±30 pptv ±18% of the measured value.

At night, a significant fraction of NO_x may be lost to NO_3 and further to N_2O_5 and HNO_3 [*Logan*, 1981; *Dentener and Crutzen*, 1993]. Under realistic conditions at the tropopause (T=-50°C, p=250 hPa) the $1/e$-lifetime of NO_2 against conversion to NO_3 is 30 days and 1.6 days assuming an O_3 concentration of 50 ppbv and 400 ppbv, respectively (reaction rates taken from *Atkinson et al.* [1997]). This gives a total conversion of 3-22% at the end of a night assuming no sunlight during ten hours. NO_x concentrations measured between December 1995 and May 1996 averaged 160 pptv during daytime and 154 pptv at night. This small difference could be due to the described nighttime loss of NO_x. However, the difference is probably biased by the somewhat different conditions during day and night (e.g., flights from the United States to Europe at night were usually made farther south than the flights from Europe to the United States during the day), which hinders an accurate quantification of the effect.

2.4. Meteorological Data and Discrimination between Tropospheric and Stratospheric Samples

Six-hourly analyses from the European Centre for Medium-Range Weather Forecasts (ECMWF) at a resolution of T213/L31 (i.e., 213 spectral components on 31 levels, corresponding in midlatitudes to a horizontal resolution of about 0.7°and a vertical resolution at the midlatitude tropopause of 800-900 m) were used to derive potential vorticity (PV) fields for the entire NOXAR and POLINAT 2 period. PV as well as other meteorological parameters (humidity, wind, potential temperature, geopotential, pressure at several different PV surfaces) were linearly interpolated in space and time to the flight tracks. The good agreement of the ECMWF analyzed winds and temperatures with the standard B-747 sensors [*Jeker et al.*, 2000] provides confidence in the ability of the model to represent the synoptic-scale structures of the tropopause.

PV is a conservative tracer under adiabatic conditions and is typically much larger in the stratosphere than in the troposphere, and on an isentropic surface the

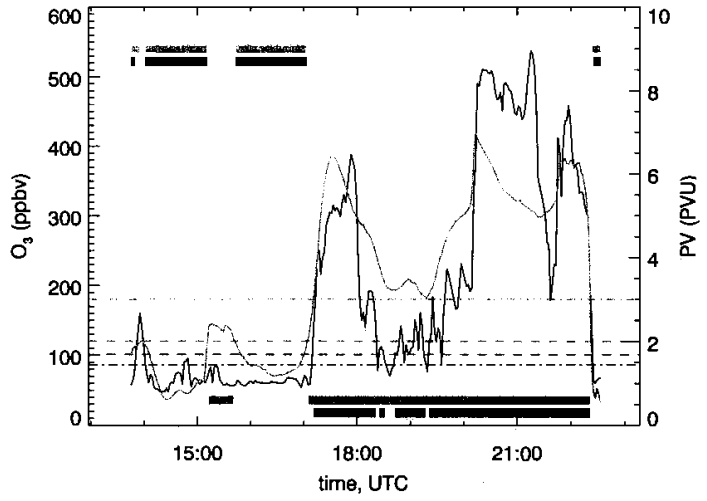

Figure 2. Ozone (solid black line) and potential vorticity (solid grey line) along the track of a flight from Zurich to Beijing on March 20, 1996. Horizontal bars denote the time spent by the aircraft in the lower stratosphere (bars at the bottom) and in the upper troposphere (bars at the top), respectively. Grey bars were derived using the "old" 2 PVU criterion. Black bars represent the new refined method. Grey horizontal lines are the 2 and 3 PVU levels. Black lines are the O_3 threshold values (dash-dotted: P_{25}(3 PVU); dashed: P_{75}(2 PVU)). See text for details.

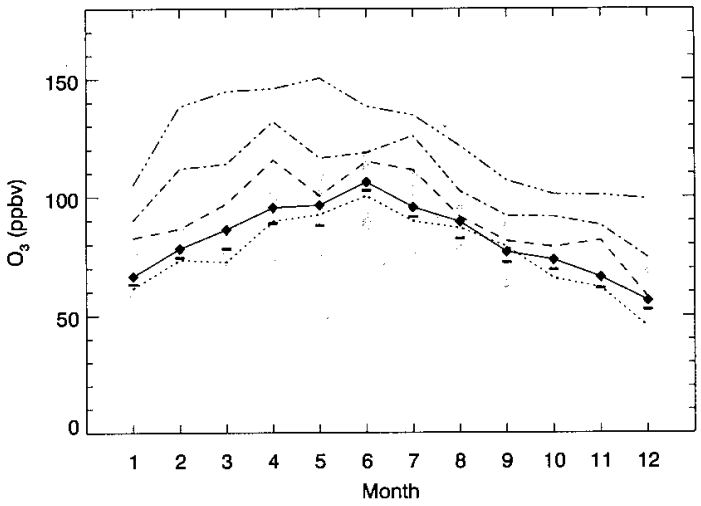

Figure 3. Seasonal cycle of the monthly mean O_3 concentration in a layer of 0.2 PVU thickness centered at five different PV surfaces. The PV surfaces corresponding to the individual lines from the bottom to the top are PV=1.6, 2, 2.5, 3, and 3.5 PVU. Grey vertical bars denote the range between the first and third quartile of the concentrations at the 2 PVU tropopause. Horizontal lines within the bars denote the median (i.e., the second quartile).

tropopause is coincident with a strong PV gradient. Potential vorticity values in the range of 1.6 and 3.5 PVU (1 PVU = 10^{-6}ms^{-1}Kkg^{-1}) have been associated previously with the dynamcial tropopause [e.g., *Hoskins et al.*, 1985; *Hoerling et al.*, 1991; *Grewe and Dameris*, 1996]. Since O_3 also increases from the troposphere to the stratosphere a well-known positive correlation between O_3 and PV is observed in the vicinity of the midlatitude tropopause [*Danielsen*, 1968; *Beekmann et al.*, 1994; *Ravetta et al.*, 1999]. Observational and theoretical studies indicate that the dynamical tropopause is in better agreement than the thermal tropopause with a tropopause defined from atmospheric tracers (e.g., the "ozone tropopause") [*Zahn et al.*, 1999; *Wirth*, 2000].

Many atmospheric tracers including O_3 exhibit a strong vertical gradient at and immediately above the tropopause, reflecting the different atmospheric regimes of the troposphere and the stratosphere with respect to transport processes and photochemistry. Since the cruising altitude of the B-747 north of about 35°N was frequently above and below the tropopause, very interesting information can be gained by separating the data set into a tropospheric and a stratospheric subsample. Following *Hoskins et al.* [1985], we applied a value of 2 PVU for the tropopause. In section 4.5, for instance, vertical profiles of NO_x and O_3 are analyzed relative to the altitude of the 2 PVU tropopause. However, in order to achieve a clear separation between tropospheric and stratospheric samples, we excluded all measurements obtained in the "tropopause region", which we define here as a transition region between the 2 and 3 PVU surfaces. Mesoscale structures are resolved by the measurements but not always by the ECMWF model and furthermore, the ECMWF analysis can sometimes be incorrect. Therefore erroneous attributions of samples can occur if we base the separation only on a PV criterion (see Figure 2). On the other hand, applying a fixed O_3 value to discriminate between tropospheric and stratospheric samples does not account for a possibly significant variability of the concentrations caused by transport and mixing processes and photochemistry. As compared to the discrimination based on the 2 PVU criterion used previously by *Brunner et al.* [1998], we here present a refined method making use of the information content of both the PV and O_3 fields. Figure 3 presents the seasonal variability of measured O_3 concentrations in a strip of ±0.1 PVU centered around five different PV levels (1.6, 2, 2.5, 3, and 3.5 PVU). Differences in O_3 concentrations between the 1.6 and 2 PVU level are only small. The seasonal cycle of O_3 at these two levels is very similar to that generally observed in the free troposphere [*Logan*, 1999] with a summer maximum. With increasing PV, the seasonal cycle more and more resembles a stratospheric cycle with an earlier maximum around April/May [*Logan*, 1999]. Thus a value of 2 PVU appears to be at the lower limit of a "tropopause region" while air at 3 PVU already reveals a distinct stratospheric character.

On the basis of this analysis we now define tropospheric and stratospheric air as follows:

$$\text{trop. air}: \ \text{PV} < 2\text{PVU}, \ O_3 < P_{75}(2\text{PVU}, t) \quad (4)$$

$$\text{strat. air}: \ \text{PV} > 3\text{PVU}, \ O_3 > P_{25}(3\text{PVU}, t), \quad (5)$$

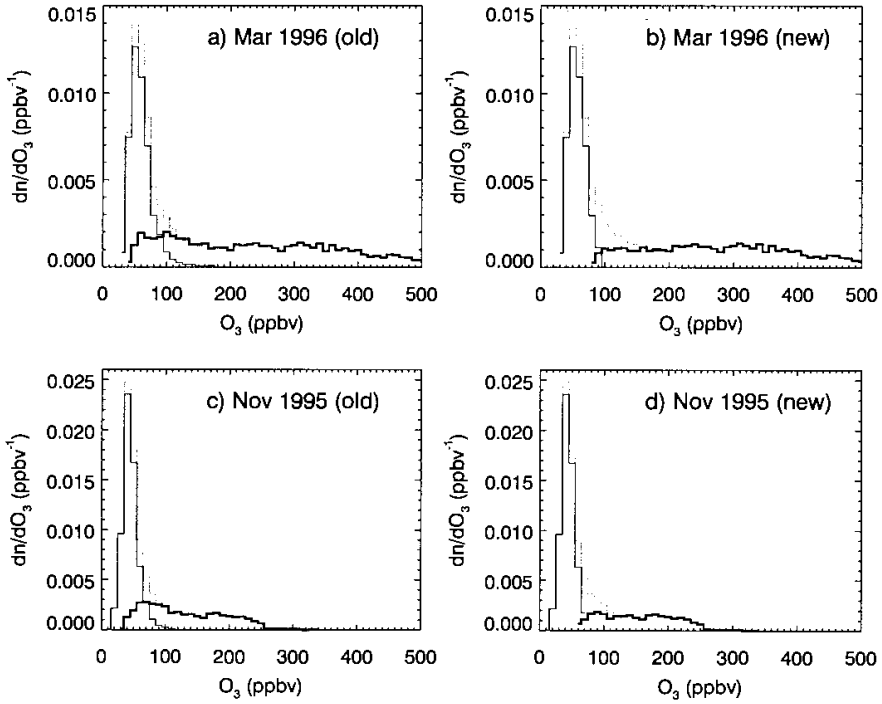

Figure 4. Probability density function of upper tropospheric O_3 concentrations in 2 separate months. The figure shows the overall (grey) and separately the tropospheric (thin black lines) and stratospheric (thick black lines) distributions. The tropospheric and stratospheric distributions were scaled by the respective fraction of samples obtained in the troposphere and the stratosphere. (a) and (c) Calculated using the "old" method based on the 2 PVU criterion. (b) and (d) Represent the results of the refined method.

where P_{75}(2PVU,t) is the 75% percentile (third quartile) of the O_3 frequency distribution at the 2 PVU surface at time t. Accordingly, P_{25}(3PVU,t) is the first quartile at the 3 PVU surface. The value of P_{25}(3PVU) is lower than P_{75}(2PVU) in all months. Upper tropospheric O_3 concentrations are thus allowed to exceed the lowest stratospheric values occasionally. The dependence on time was determined by fitting a fourth-order polynomial to the monthly quartiles. By this definition we eliminate air samples with very large O_3 below the 2 PVU surface and very low O_3 above the 3 PVU surface, which could be attributable to errors in the ECMWF analysis or to none-resolved small-scale structures. Six and three-tenths percent of all measurements at cruising altitudes could not be attributed to either the troposphere or the stratosphere using the above criteria.

The improvement of the separation between tropospheric and stratospheric samples applying the new method is demonstrated for an exemplary flight in Figure 2. Figure 4 shows the frequency distributions of tropospheric and stratospheric samples separated according to the refined and the "old" methods for two seasons. This demonstrates the better separation at the tropopause level, whereas the overall shape of the distributions is almost unchanged with the new method.

3. Overview of the Measurements

3.1. Temporal and Spatial Coverage

The NOXAR system was operating on a total of 623 flights between Zurich, Switzerland, and various destinations in the United States and the Far East (Figure 5). The first observation period extended from May 5, 1995, until May 13, 1996 (540 flights). The instrumentation was flown for another 104 days from August 12 until November 23, 1997, in the framework of POLINAT 2. The majority of flights (83) in 1997 were performed between Zurich and the United States, and only these are included here. The measurements covered a wide range of latitudes (15°-65°N) and longitudes (90°W-120°E) in the northern hemisphere, but roughly three quarters of all samples were obtained in midlatitudes between 30°and 60°N. A total of 3798 hours of O_3 and 2052 hours of NO_x data was sampled. The lower coverage of NO_x is due to (1) frequent background/zero checks and regular calibrations, (2) instrumental failures, particularly of NO_2, (3) many nighttime flights

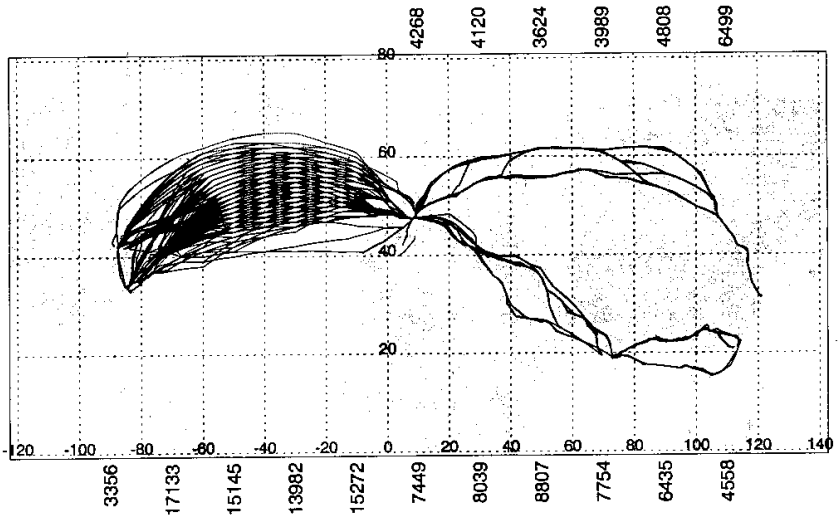

Figure 5. Flight tracks of the B-747 during NOXAR (1995/1996) and POLINAT 2 (1997). The home base is Zurich. The main destinations in the United States were Atlanta, Boston, New York, and Chicago and in the Far East Beijing, Bombay, and Hong Kong. Individual lines typically represent many individual flights following the same track. Over the North Atlantic the flight corridors may be shifted north-southward depending on current weather conditions. Flights to the United States usually followed a more northern track than return flights to Europe to avoid and make use of the jet stream. The number of 2-min integrated data samples obtained per 20° longitude section is indicated at the top (flights to Beijing) and at the bottom of the figure (flights to the United States and to Bombay - Hong Kong), respectively.

with missing NO_2 data, and (4) the dismissal of data before the first and last zerocheck on each flight.

3.2. Fractional Cruising Time in the Stratosphere

The relative time spent by an aircraft in the LS and the UT is important considering the potentially different effects of the emissions on the background concentration levels and photochemistry. *Gettelman and Baughcum* [1999] (hereafter referred to as GB99) estimated that between 18% and 44% of current aircraft exhaust emissions are deposited in the stratosphere, depending on the season and on the exact definition of the tropopause. In the North Atlantic flight corridor it is estimated that about 44% of aircraft cruising time is accomplished in the LS [*Hoinka et al.*, 1993].

Figure 6 shows the seasonal cycle of the fractional cruising time of the B-747 in the stratosphere (shaded area) for flights between Zurich and the destination in the United States. Individual lines in the figure represent the fraction of cruising time spent below a given value of potential vorticity. Although this result was derived for a single airplane only, it is probably typical for flights between Europe and the United States. The annual average of stratospheric cruising time of 48% agrees fairly well with the estimate of *Hoinka et al.* [1993], although their analysis was restricted to a somewhat smaller geographical domain and was obtained for a lower tropopause of 1.6 PVU. A marked seasonal cycle can be seen in the figure which is a consequence of the seasonal variation of tropopause pressures in midlatitudes [*Hoinka*, 1998; *Appenzeller et al.*, 1996]. GB99 analyzed the stratospheric fraction of aircraft fuel use and emissions using global aircraft emissions inventories with different reanalysis data sets of tropopause pressures. Although their results represent global air traffic including flights in the Southern Hemisphere, they found a very similar seasonal dependence of the fraction of stratospheric fuel use (a maximum in February and a minimum in August) as the one observed over the North Atlantic in Figure 6. This good agreement is due to the fact that a large proportion of global air traffic occurs at northern midlatitudes between 30°and 60°N. GB99 found a strong latitudinal dependence of the fractional fuel use in the stratosphere, which is the result of the north-south gradient in mean tropopause altitudes. Flights of the B-747 to Beijing were carried out on average further north than flights to the United States (see Figure 5) and were therefore located predominantly in the stratosphere. Flights to Bombay, on the other hand, were mainly in the troposphere, in particular to the south of the subtropical jet stream. Flights between Bombay and Hong Kong were carried out almost exclusively in the troposphere.

Ninety-five percent of all NOXAR samples were obtained at potential temperatures lower than 350 K.

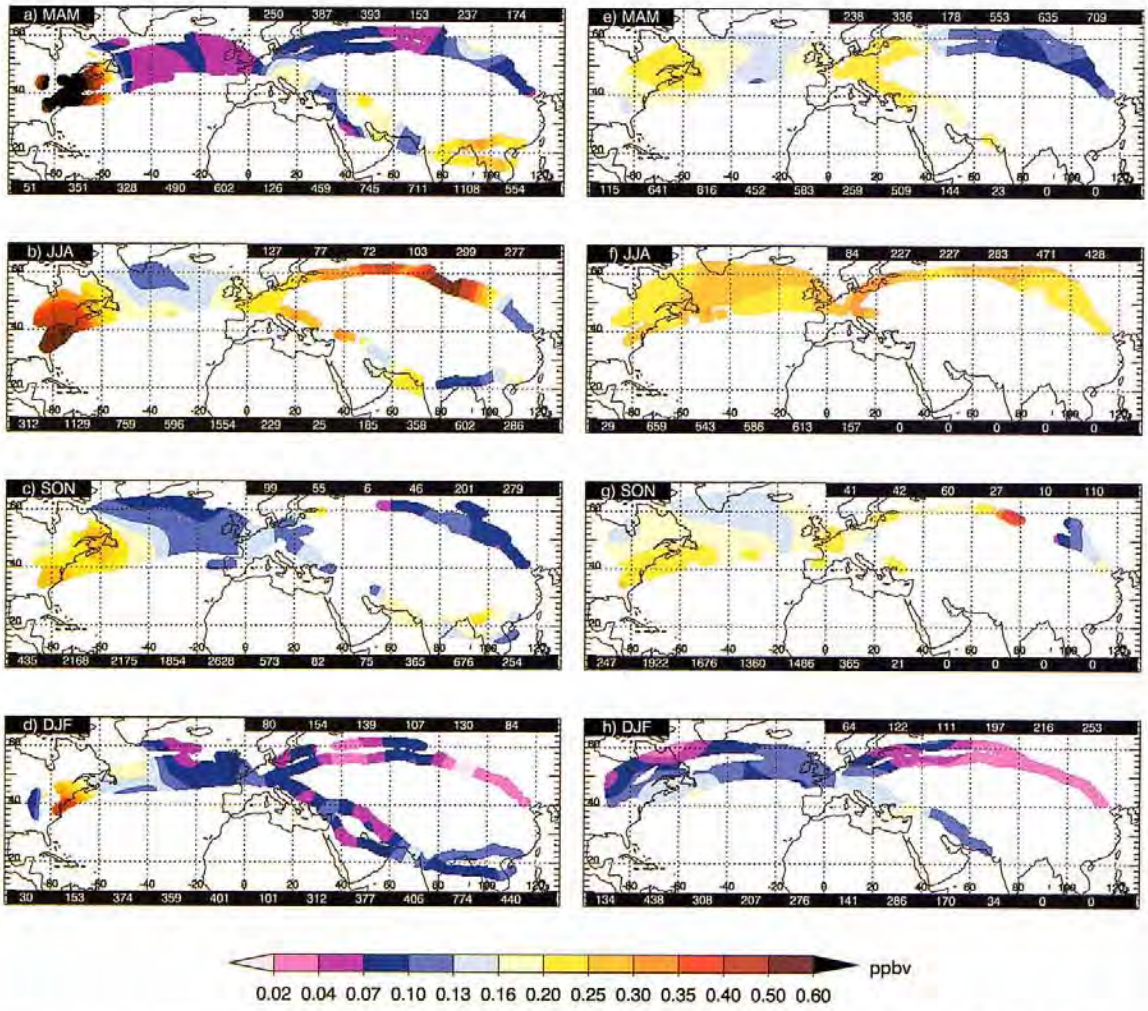

Plate 1. Distribution of NO_x in the 330-200 hPa altitude range in the four seasons spring (MAM), summer (JJA), autumn (SON) and winter (DJF) filtered with a 2-D Gaussian filter of half-width $\sigma = 3°$. (left) Upper tropospheric samples. (right) Lower stratospheric samples only. Numbers denote the sample size in individual 20° longitude sections for flights ZH - Beijing (top) and for flights ZH - United States, ZH - Bombay, and Bombay - Hong Kong (bottom).

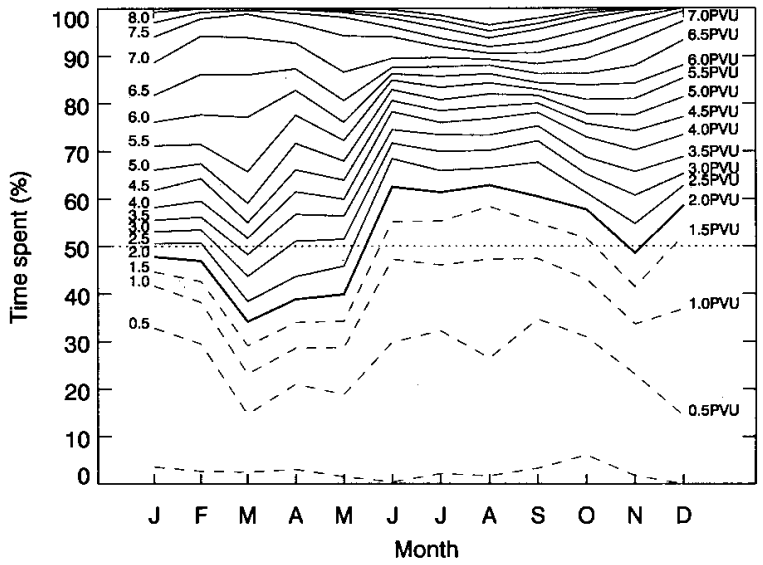

Figure 6. Seasonal variation of the fractional cruising time (in %) spent by the NOXAR B-747 between Zurich and U.S. destinations below a given value of potential vorticity (PV). The PV values (in PVU) are indicated to the left and right of the corresponding lines. Only measurements in the altitude range 330-200 hPa (approximately 8.6-11.8 km)were considered. The shaded area represents the stratospheric fraction for a tropopause at 2 PVU.

Thus all stratospheric flights took place in the "lowermost stratosphere" defined by Holton et al. [1995] as the part of the stratosphere between the tropopause and the 380 K potential temperature surface. Since isentropes below the 380 K level intersect the tropopause, air in the lowermost stratosphere can mix isentropically into the UT and therefore has a rather short stratospheric residence time. *Gettelman* [1998] estimated that the $1/e$-folding residence time of subsonic aircraft emissions in the LS is on the order of 50 days.

4. Results and Discussion

In this section a "climatology" of the distributions of NO_x and O_3 is presented, using all measurements obtained at cruising altitudes between 8500 m and 11,600 m (330-200 hPa). To account for the different chemical and dynamical regimes of the troposphere and the stratosphere, we discriminate between samples obtained in the UT and the LS as described in section 2.4. O_3 has a very long lifetime in the LS, and consequently its distribution is mainly determined by dynamical processes. In section 4.4 we therefore additionally present the O_3 concentrations in a dynamically consistent framework as a function potential vorticity and potential temperature. Tropopause-scaled vertical profiles of NO_x and O_3 relative to the 2 PVU tropopause are presented in section 4.5.

4.1. NO_x Distribution at Cruising Altitudes

4.1.1. Seasonal mean distributions. The horizontal distribution of NO_x in the four seasons is shown in Plate 1, separately for the UT and the LS as defined by equations (4) and (5). The distributions were filtered with a horizontal (2D) Gaussian filter (half-width $\sigma = 4°$) as described by *Brunner* [1998] in order to better reveal the large-scale features of the distributions by suppressing smaller than synoptic-scale structures. Plate 1 is similar to Figure 3 of *Brunner et al.* [1998], but additional data have been included here, and a refined method was applied to better discriminate between the UT and the LS. The total number of 2-min samples in the present (previous) study is 16,309 (8411) in spring, 13,534 (12,042) in summer, 22,579 (11,181) in autumn, and 9169 (4423) in winter. The overall picture changes only little compared to *Brunner et al.* [1998] suggesting a certain degree of robustness of the results to the exact definition of the tropopause and the amount of data included. The dominant features in the UT (Plates 1a-1d) are a pronounced maximum over the east coast of the United States in spring and summer, and a broad maximum extending from Europe to Siberia in summer. These maxima are associated with the frequent occurrence of large-scale NO_x plumes downwind of thunderstorms and frontal systems as described previously by *Brunner et al.* [1998] and *Jeker et al.* [2000]. The maxima are absent in the strato-

spheric maps (Plates 1e-1h) because almost no such plumes were observed above the tropopause. In general, the distributions are zonally much more uniform in the LS than in the UT, which is consistent with the expected longer lifetime in the LS [*Schumann*, 1994]. The stratospheric concentrations usually exceed the tropospheric values except for the upper tropospheric maxima over the continents associated with the frequent occurrence of large-scale plumes. Nitrogen oxides in the stratosphere are formed mainly at altitudes of 30-40 km through the decomposition of nitrous oxide (N_2O) and are transported downward by the Brewer-Dobson circulation.

The impact of aircraft emissions on background concentrations is expected to be larger in the LS than in the UT, due to the differences in lifetime [*Schumann*, 1994]. The lower stratospheric NO_x concentrations are distinctly higher over the North Atlantic region than over Siberia during winter and spring, which may be attributable to different amounts of air traffic emissions. Consistent with this interpretation, the ANCAT air traffic emissions inventory [*Gardner*, 1998] predicts about a factor of 4 to 10 times higher emissions over the North Atlantic region than over Siberia. However, a similar contrast between the two regions is not observed in summer when the concentrations are generally higher than in winter/spring. These differences between summer and winter are in agreement with results from model calculations indicating the strongest impact of aircraft NO_x emissions on background levels during winter [*Brasseur et al.*, 1998; *Dameris et al.*, 1998; *Lamarque et al.*, 1996].

An indication for a larger impact of aircraft emissions in the LS than in the UT is provided by the observations of short high NO_x spikes. These spikes are most probably attributable to exhaust emission plumes from other aircraft flying ahead of the Swissair B-747. Exemplary observations of such plumes were presented previously by *Dias-Lalcaca et al.* [1998] and *Brunner et al.* [1998]. A detailed description of similar spikes observed from the DLR Falcon aircraft and their attribution to aircraft exhaust plumes was presented by *Schlager et al.* [1997]. During NOXAR, 1340 such spikes were observed in midlatitudes (40°to 60°N) with concentrations ranging from 0.5-10 ppbv and extending 1-10 3-s samples (that is about 750 m to 7.5 km) along the flight track. 11.6% of all 2-min samples in the LS were affected by spikes in the LS, and 10.5% in the UT. However, the plumes were on average higher in the LS, and, consequently, their effect on the calculated mean concentrations was larger. By including and excluding samples obtained in such plumes, their annually averaged contribution to the NO_x concentrations in midlatitudes (40°to 60°N) was estimated to 31 pptv in the LS and only 20 pptv in the UT. The overall fraction of the NO_x abundance in the UT and the LS made up by such aircraft exhaust plumes is most probably overestimated in the NOXAR observations because the B-747 was restricted to the same flight levels as the other airliners and was crossing the North Atlantic flight corridor during peak traffic hours.

Accounting for the amount of NO_x contained in the plumes provides only a course estimate of the overall contribution from air traffic at cruising altitudes, since a large fraction of the emitted NO_x is expected to be mixed with the background. The lifetime of NO_x is probably of the order of several days at the tropopause [e.g., *Jaeglé et al.*, 1998], which exceeds the 3 to 10 hours required to mix such plumes homogeneously with the background [*Schumann et al.*, 1998].

4.1.2. Frequency distributions. Figure 7 shows the frequency distributions of NO_x in the UT and the LS in the four seasons for three different regions: Europe/Asia, 35°-65°N, 0°-120°E (Figure 7a); North America, 35°-60°N, 60°-100°W (Figure 7b) ; North Atlantic, 40°-60°N, 10°-40°W (Figure 7c). The North Atlantic box is located over the eastern part of the Atlantic. Its western border is approximately 2000 km downwind of major surface emission sources along the U.S. east coast. The North American region actually covers only the east coast of the United States and parts of Canada. This region and the Europe/Asia area are expected to be much more strongly affected by continental surface emissions. Also lightning emissions are far larger over the continents [*Price and Rind*, 1992].

In general, the frequency distributions can be well approximated by a lognormal behavior. Significant deviations from this behavior are associated with comparatively poor statistics, e.g., over North America in MAM and DJF. Typical distributions are thus characterized by a long tail toward high concentrations and by mean values, which distinctly exceed the respective medians.

A summary of mean and median values obtained in the different regions is given in Table 1. Note that for a lognormally distributed quantity c the distribution dN/dc is fully determined by the mean $E(c)$ and median $M(c)$ [e.g., *Seinfeld and Pandis*, 1998]:

$$\frac{dN}{dc} = \frac{1}{c\sigma\sqrt{2\pi}} \exp\left(-\frac{1}{2}\left(\frac{\ln c - \ln M}{\sigma}\right)^2\right), \quad (6)$$

where σ is the standard deviation of $\ln(c)$. For a lognormal distribution, σ is given by $\sigma = 2\sqrt{\ln E - \ln M}$.

The stratospheric distributions (thin lines) are quite similar in the different regions for a given season. They show a pronounced seasonal cycle with largest values in summer and lowest in winter. This behavior can be partly understood by the tendency of NO_x in the LS to achieve a photostationary equilibrium with NO_y [*Kawa et al.*, 1993; *Gao et al.*, 1997]. The larger amount of sunshine during summer converts a larger fraction of total reactive nitrogen NO_y into NO_x. In winter, not only the less intense sunlight but also heterogeneous conversion to HNO_3 efficiently reduces the amount of NO_x [*Dentener and Crutzen*, 1993; *Gao et al.*, 1997].

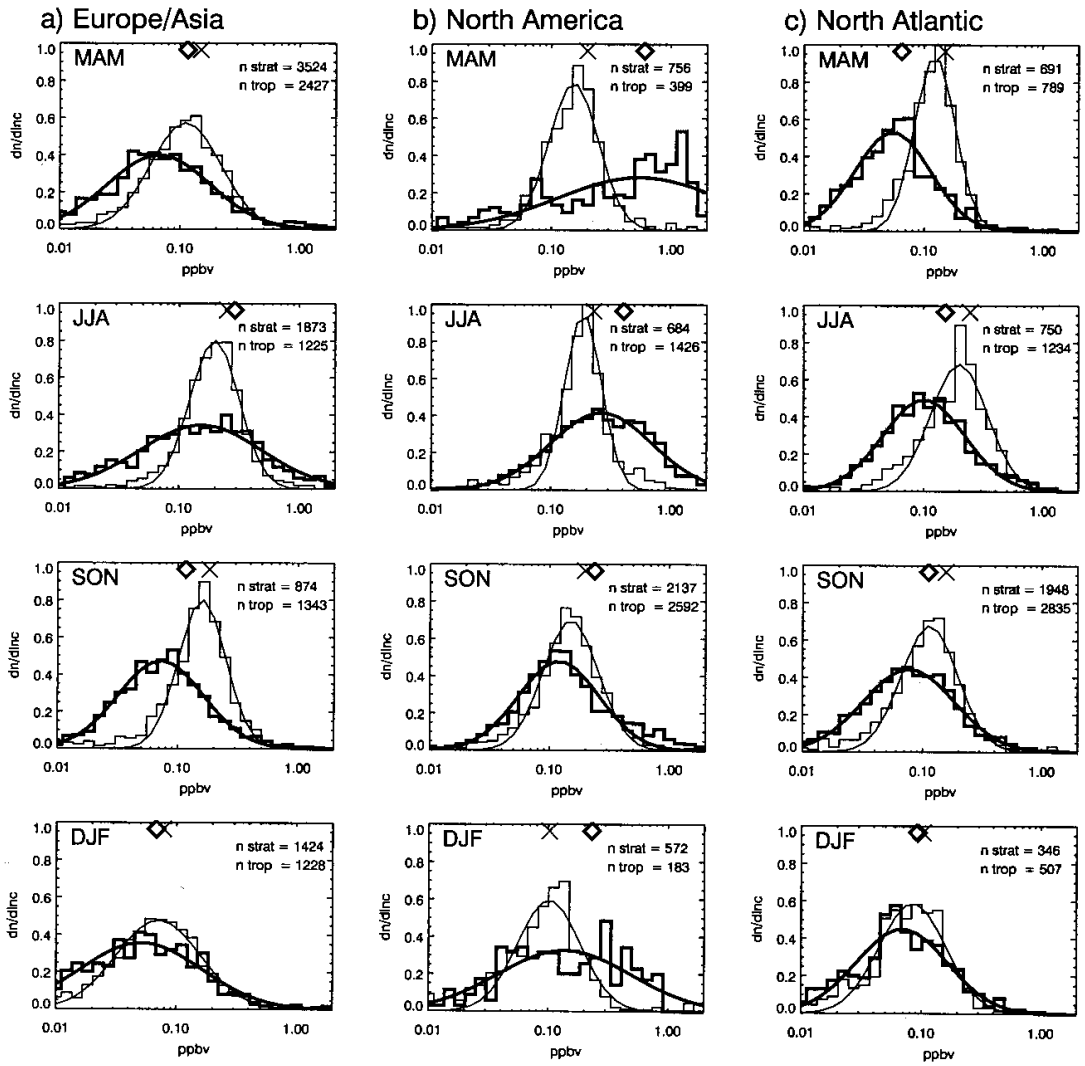

Figure 7. Probability density distributions ($dn/d\ln[NO_x]$) of the logarithm of the NO_x concentration in the four seasons. (a) Europe/Asia: 40°-65°N, 10°-120°E. (b) Eastern North America: 35°-60°N, 60°-100°W. (c) North Atlantic: 40°-60°N, 10°-40°W. Thick lines: Tropospheric samples. Thin lines: stratospheric samples. Also shown are lognormal fits to the distributions (smooth curves). Diamonds and crosses denote the mean values in the upper troposphere and the lower stratosphere, respectively. The number of 2-min samples in the stratosphere and the troposphere is indicated in the top right corner of each plot. Note: Negative concentrations, which can occur due to the limited precision of the instruments, were excluded in this representation and the calculation of the lognormal fit. There is therefore some discrepancy between the Figure and Table 1 in seasons and over regions with low average concentrations and thus a significant fraction of negative values.

This is likely the reason for the observed decrease in NO_x concentrations toward high latitudes in winter as seen in Plate 1.

The tropospheric distributions (thick lines) are typically much broader indicating that they stem from a different population. The increased variability points toward a balance between larger sources and sinks in the UT as compared to the LS [*Jobson et al.*, 1999]. Only during winter the distributions in the UT and the LS are quite similar, except over North America. Aircraft emissions, which occur in comparable amounts above and below the tropopause (compare Figure 6), are possibly dominating the distributions during winter. As opposed to the stratospheric distributions, the tropospheric ones are remarkably different between the three selected regions. The highest concentrations in the UT

Table 1. Characteristics of Probability Density Distributions of NO_x Over Three Regions.[a]

		Europe/Asia			North America			North Atlantic			Southeast Asia		
	Season	n	$E(c)$	$M(c)$	n	$E(c)$	$M(c)$	n	$E(c)$	$M(c)$	n	$E(c)$	$M(c)$
Overall	MAM	7,298	136	94	1,311	323	175	1,850	103	85	2,005	238	147
	JJA	3,905	264	199	2,505	351	231	2,317	185	140	964	120	83
	SON	2,278	140	101	5,371	218	151	5,529	131	96	1,060	179	117
	DJF	3,325	74	45	824	139	91	943	95	70	1,477	107	97
	YEAR	16,806	154	101	10,011	259	165	10,639	135	99	5,506	171	118
Stratosphere	MAM	3,524	149	117	756	200	169	691	151	133	...	...	...
	JJA	1,873	250	216	684	230	204	750	244	217	...	...	...
	SON	674	184	166	2,137	197	160	1,948	156	121	...	...	...
	DJF	1,424	78	56	572	102	80	346	102	86	...	...	...
	YEAR	7,495	164	133	4,149	190	159	3,735	178	132	...	...	...
Troposphere	MAM	2,427	116	58	399	603	392	789	65	48	1,904	239	146
	JJA	1,225	290	151	1,426	407	278	1,234	152	106	962	118	83
	SON	1,343	117	77	2,592	237	134	2,835	111	72	1,041	177	115
	DJF	1,228	68	25	183	230	122	507	92	61	1,406	102	93
	YEAR	6,223	141	66	4,600	321	172	5,365	112	73	5,313	169	115

[a] $E(c)$ is the mean concentration (pptv), $M(c)$ is the median (pptv), and n is the number of 2-min averaged samples.

were observed over North America in all seasons, followed by the Europe/Asia region. In spring and summer, average tropospheric concentrations over North America strongly exceeded the corresponding stratospheric values. Contrastingly, the concentrations over the North Atlantic were generally lower in the UT than in the LS. The Europe/Asia regions is somewhere in between these two extremes. Its distributions significantly differ from the North Atlantic distributions only during spring and summer.

The long tails toward high concentrations observed in the upper tropospheric distributions over the continents is a direct consequence of the frequent occurrence of large-scale convection/lightning plumes as described by *Brunner et al.* [1998]. The spring distribution over North America is strongly dominated by observations in a few such plumes. Because the statistics of these events is rather poor, the distribution can not be regarded as being representative for spring conditions over North America. Nevertheless, springtime and summer concentrations in the UT over the east coast of the United States appear to be dominated by strong local sources, which probably consist of a combination of lightning activity and convective transport of surface pollutants from the densely populated coastal areas. Different from the North American region, a distinct local continental influence over Europe/Asia is only visible during spring and and particularly during summer.

4.1.3. Seasonal cycle. The seasonal variation of NO_x concentrations over the three regions (North America, Europe/Asia, and North Atlantic) and over a third region between Bombay and Hong Kong is shown in Figure 8. The figure further emphasizes the differences between the upper tropospheric NO_x concentrations (dotted lines) over the continents (Figures 8a and 8b) and over the North Atlantic (Figure 8c): The seasonal cycle in the UT is rather flat over the North Atlantic with a minimum in April and a maximum in August. Over Europe/Asia, however, there is a pronounced maximum between June and August and a minimum in winter with comparable concentrations as over the North Atlantic. The high values during summer are associated with a strongly increased variability. Very high values were observed over North America in April and May, as discussed in the previous section. The stratospheric seasonal cycles (dashed lines) are again quite similar between the three regions. The solid line is the overall mean concentration, which falls between the tropospheric and stratospheric values according to the fractional cruising time in the stratosphere.

The seasonal cycle between Bombay and Hong Kong (Figure 8d) shows a different behavior. Since no stratospheric air was sampled on these flights, no distinction could be made between the UT and the LS. Two maxima can be discerned, the first one in spring and the second in autumn. Both were associated with increased variability as indicated by the vertical bars. The local minimum between June to August is rather surprising as is coincides with the period of the Asian summer Monsoon, which is associated with intensive convective activity over India and Bangladesh. In contrast to the observations, many CTMs calculate a distinct maximum over this region in summer caused by lightning activity [*Brasseur et al.*, 1998; *Berntsen et al.*, 1999]. As shown later, O_3 concentrations were also low during July and August. This unexpected result is probably due to a combination of several effects. Convection may inject air masses depleted in O_3

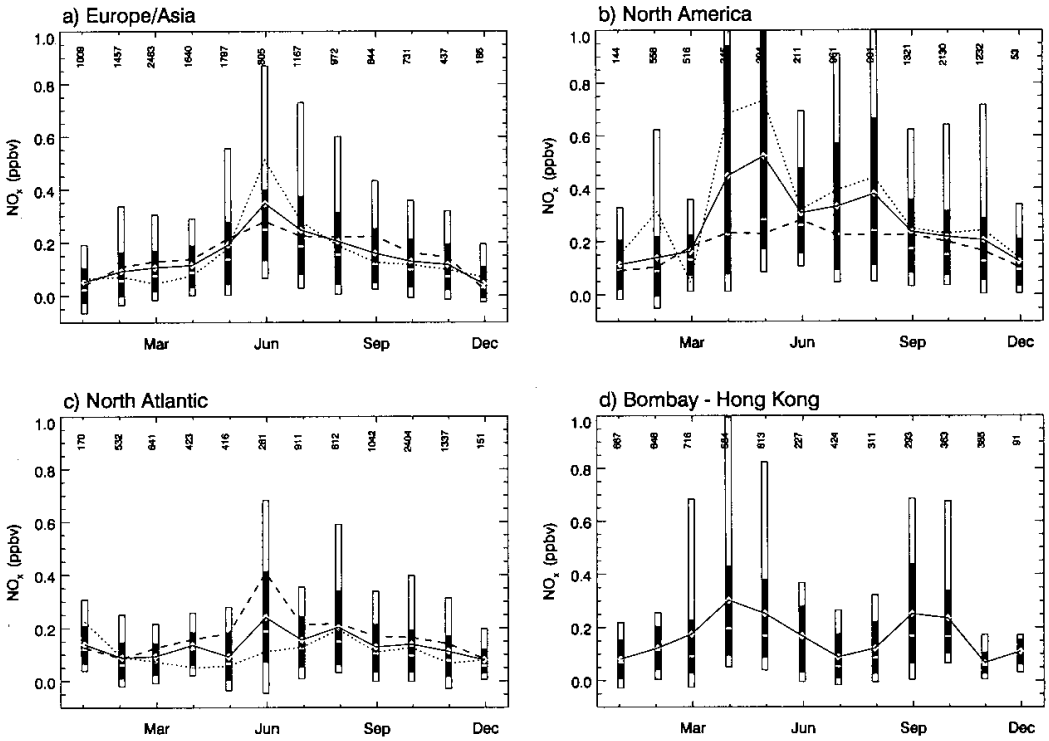

Figure 8. Seasonal cycle of NO_x concentrations in the 330-200 hPa range. Vertical bars denote the variability in each month. Inner (grey) boxes represent central 67% (P_{16}-P_{83}, outer boxes central 90% (P_5-P_{95}) percentiles. Mean values are connected by lines. Solid lines: all samples. Dashed lines: stratospheric samples only. Dotted lines: tropospheric samples only. Horizontal bars denote median values. (a) Europe/Asia: 40°-65°N, 10°-120°E. Value off-scale in June: 2.67 ppbv (P_{95}). (b) Eastern North America: 35°-60°N, 60°-100°W. Values off-scale in April: 1.68 ppbv (P_{95}); in May: 1.01 (P_{83}), 1.50 (P_{95}); in August: 1.12 (P_{95}). (c) Eastern North Atlantic: 40°-60°N, 10°-40°W. (d) Southeast Asia between Bombay and Hong Kong: 10°-30°N, 70°-120°E.

and other trace gases from lower altitudes [*Lelieveld and Crutzen*, 1994]. Ground stations over India indeed report the lowest NO_x and O_3 concentrations during summer [*Naja and Lal*, 1996; *Kulshreshta et al.*, 1997]. Furthermore, the combination of high temperatures and humidity, and the world's highest precipitation rates promote the rapid removal of O_3 and NO_x through oxidation by OH and, in the case of NO_x, wet deposition of the oxidation product HNO_3. The missing lightning NO_x may be explained with the hypothesis that only a small part is deposited at cruising levels. Convective towers reach up to the tropopause located at 16 to 18 km over India during summer. In a recent study on the vertical distribution of NO_x produced by lighting in thunderstorms, *Pickering et al.* [1998] concluded that the largest fraction is deposited some 2 to 4 km below the tropopause. In the tropics during summer these altitudes are well above the cruising levels of civil airliners. The NOXAR observations support this picture as they reveal a very strong increase in NO_x with altitude. Mean concentrations (and central 67%) in JJA at the three main cruising levels at 8600 m, 10,030 m, and 11,270 m were 54 pptv (0-83 pptv), 106 pptv (16-192 pptv), and 186 pptv (75-282 pptv), respectively. Another possible explanation for some of the "missing" lightning NO_x is that airliners try to avoid flying in the vicinity of large convective towers where the highest concentrations would be expected.

4.2. O_3 Distribution at Cruising Altitudes

4.2.1. Seasonal mean distributions. Plate 2 shows maps of the O_3 distributions in the UT (Plates 2a-2d) and the LS (Plates 2e-2h) defined according to equations (4) and (5). As expected, the concentrations in the LS are much higher than in the UT. Note that the exact definition of the tropopause has quite a significant impact on the absolute concentrations in the lower stratosphere, which is a consequence of the strong vertical gradient of O_3 at and immediately above the tropopause. There is no correlation between the geographical patterns in the UT and the LS suggesting that the discrimination between the two atmospheric regimes

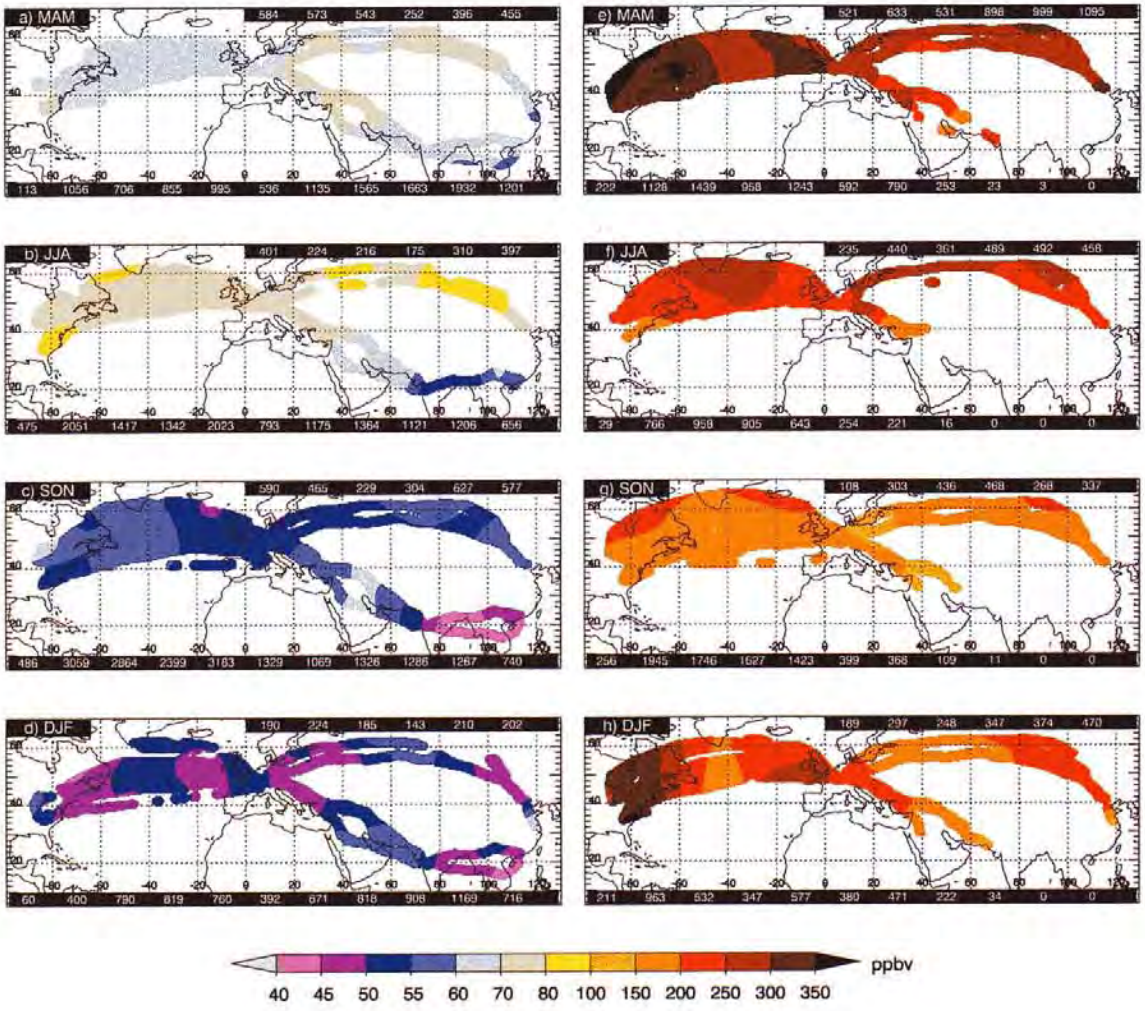

Plate 2. Same as Plate 1, but for ozone.

applying equations (4) and (5) is very successful. The distributions in the LS are controlled by geographical differences in the seasonal mean tropopause altitude which is governed by large-scale dynamical processes. The maxima over eastern North America and northeastern Asia in winter and spring for instance, are related to the well known quasi-stationary troughs associated with Rossby waves downwind of the Rocky Mountains and the Himalayas [*Holton*, 1992]. A comparison of the seasonal mean weather pattern during the NOXAR period with a 10-year (1979-1988) climatology [*Brunner*, 1998] revealed that the main features of the distributions of geopotential and potential vorticity at the 250 hPa level were well represented in 1995/1996. The largest deviation from the climatological average was seen over Europe during winter. This was related to the very low North Atlantic Oscillation (NAO) index in this winter (an update of NAO indices presented by *Hurrell* [1995] can be found at http://www.cgd.ucar.edu/cas/climind/nao_winter.html). The pronounced pattern in DJF (Plate 2h) low O_3 values over the central North Atlantic and high values near Europe is most likely a direct consequence of this. Seasonal differences in lower stratospheric ozone agree well with the observations from the MOZAIC program [*Thouret et al.*, 1998], although their discrimination between tropospheric and stratospheric air was based on a threshold of 100 ppbv. The seasonal cycle will be discussed in more detail in the following section.

Different from NO_x, upper tropospheric O_3 (Plates 2a-2d) shows only a minor zonal variability. This is consistent with the comparatively long lifetime of O_3 against chemical destruction of the order of months [*Roelofs et al.*, 1997]. Consequently, the O_3 distribution does not show a strong contrast between the continents and the North Atlantic region as observed in NO_x. During spring and summer, however, there are indications for somewhat enhanced concentrations over the continents (compare next section). This is in agreement with the previously reported observations of on average higher O_3 concentrations within large-scale NO_x plumes than outside and the more frequent occurrence of the plumes over and downstream of the continents [*Brunner et al.*, 1998]. In midlatitudes, no clear pattern can be identified with respect to a north-south gradient in upper tropospheric O_3 concentrations. A distinct meridional gradient is only visible on flights between Zurich and Bombay in the vicinity of the subtropical jet stream. Seasonal differences in the midlatitude UT with typical values in the range of 45 to 55 ppbv in winter and 70 to 90 ppbv in summer are in very good agreement with results obtained by the MOZAIC program [*Thouret et al.*, 1998].

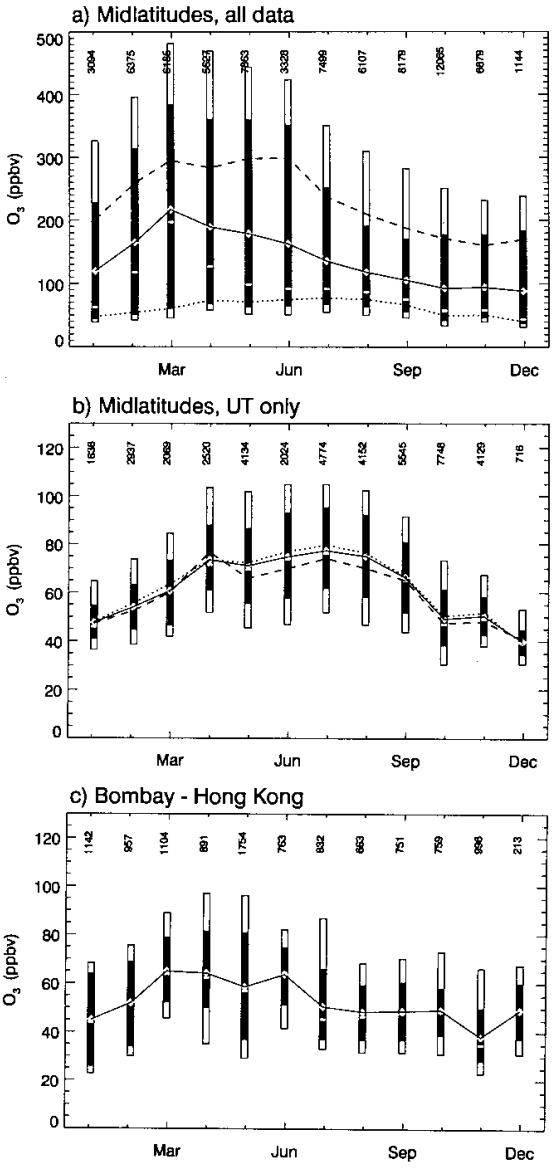

Figure 9. Seasonal cycle of O_3 in the 330-200 hPa range. For definition of symbols and geographical domains, see Figure 8. (a) Midlatitudes. Solid line: all samples. Dashed line: stratopheric samples only. Dotted line: tropospheric samples only. (b) Midlatitudes, tropospheric samples only. Solid line: all samples (same as dotted line in Figure 9a). Dotted line: samples over the continents (North America and Europe/Asia) only. Dashed line: samples over the North Atlantic only. (c) Southeast Asia between Bombay and Hong Kong.

4.2.2. Seasonal cycle. The seasonal variation of O_3 in the UT and the LS in midlatitudes and between Bombay and Hong Kong is shown in Figure 9. In the LS (dashed line in Figure 9a) the cycle is dominated by the seasonal variation in monthly mean tropopause altitudes and, as will be shown in section 4.4, by the seasonal variation in lower stratospheric O_3 caused by the Brewer-Dobson circulation. The maximum is reached in spring between March and June and the minimum in late autumn. A distinctly different seasonal cycle is

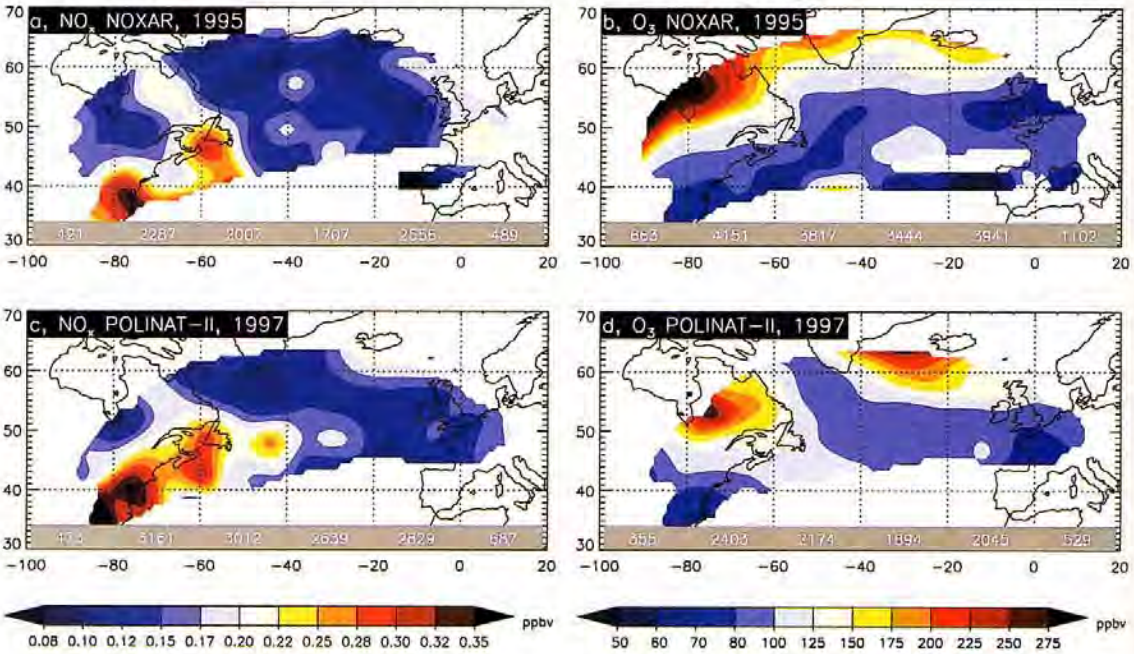

Plate 3. Maps of the NO_x and O_3 distribution in the time period August 13 to November 23 in 1995 (top) and in 1997 (bottom). The plates were created in the same way as Plates 1 and 2 but using a more narrow Gaussian low-pass filter of half-width 2°.

found in the UT (Figure 9b). Here a broad maximum exists between June and August associated with the seasonal cycle in tropospheric photochemical activity. A similar behavior has been reported previously for observations in the free troposphere from balloon soundings [*Logan*, 1985, 1999]. Figure 9b shows the seasonal cycle separately for the North Atlantic (dashed) and the North American (dotted) regions. The concentrations are 5 to 10 ppbv higher over the continents than over the North Atlantic between May and August, indicating enhanced insitu photochemical O_3 production or transport of elevated O_3 levels from the continental boundary layer to the free troposphere.

The seasonal cycle on the route between Bombay and Hong Kong is again very different from the midlatitude regions (Figure 9c). A maximum is found between March and May. The proximity to the subtropical jetstream during this time of the year and the similarity to the seasonal cycle in the midlatitude LS suggest a link between the midlatitude LS and the tropical to subtropical UT. Enhanced O_3 concentrations in the tropical UT associated with transport of stratospheric air across the subtropical tropopause break have been reported previously [*Cammas et al.*, 1998; *Zachariasse et al.*, 2000]. Between June and August there was a drop in O_3 concentrations which was accompanied by a sharp reduction in NO_x. The close relation of this feature with the Asian summer Monsoon was discussed earlier.

4.3. Differences Between 1995 and 1997

Considering the high variability of NO_x and the inherently limited spatial and temporal coverage of measurements from an airplane, the representativity of the NOXAR data is in question. Additionally, the fact that the monthly mean NO_x concentrations may vary by more than 15% from year to year [*Sausen and Köhler*, 1994] puts a limit to the representativity of the observations in a climatological sense. To address these questions we consider the time period August 13 to November 23 for which observations from two different years are available: 1995 (NOXAR) and 1997 (POLINAT 2).

Plate 3 compares the geographical distribution of NO_x and O_3 between Europe and North America in the 2 years. The NO_x distributions (Plates 3a and 3b) show remarkable similarities with enhanced concentrations near the east coast of the United States and a minimum over the central and eastern Atlantic. Only in 1995, elevated concentrations were also observed over Europe. The maximum over the U.S. east coast in 1997 was associated with several large-scale plumes as described by *Jeker et al.* [2000]. Lightning activity triggered over the warm Gulf Stream was found to be an important source for the regional upper tropospheric NO_x budget.

Figure 10 shows the corresponding frequency distributions of all NO_x and O_3 observations obtained be-

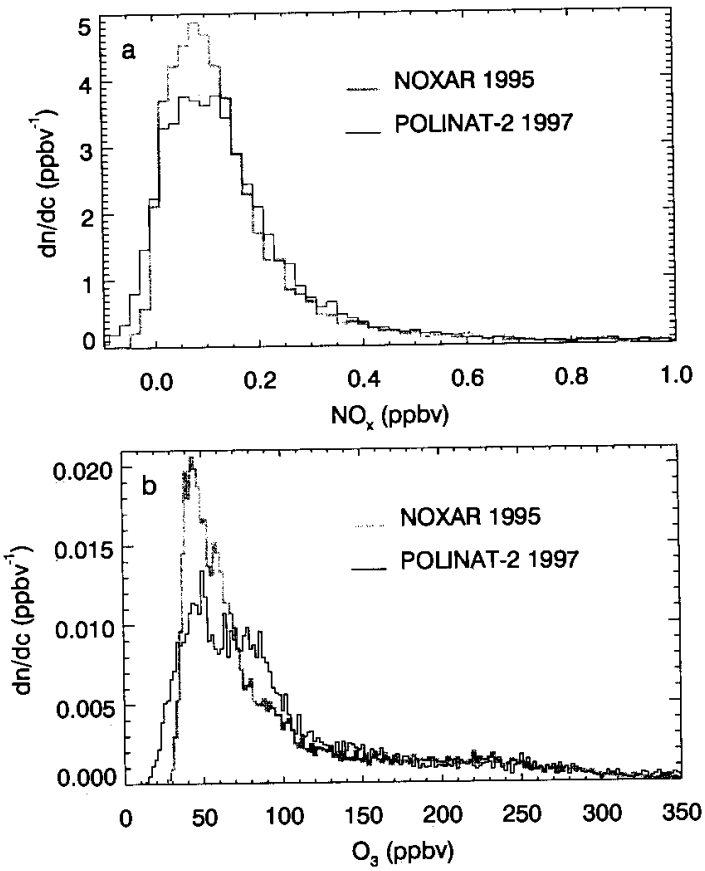

Figure 10. Probability density distributions of all samples obtained on flights between Zurich and the United States in the time period of August 12 to November 22. (a) NO_x. (b) O_3. Thick lines: 1995 (NOXAR). Thin lines: 1997 (POLINAT 2).

tween Europe and the United States. Both the overall shape of the distributions and the mean and median concentrations were similar in the 2 years. Mean/median values were 174/120 pptv in 1995 and 192/130 pptv in 1997.

The distributions of O_3 (Plates 3c and 3d) in the 2 years reveal some similarities and also some significant differences. In both years the concentrations increased toward high latitudes, and the range of observed seasonal mean values was similar. Since O_3 concentrations at cruising levels are very sensitive to the tropopause altitude, the differences are probably related to differences in the specific weather conditions between the two years. Not only the geographical distributions but also the frequency distributions show clear differences (Figure 10b). The 1997 data show a considerable number of very low O_3 concentrations below 30 ppbv. *Grant et al.* [2000] reported on observations of very low O_3 concentrations (down to 18 ppbv) over the North Atlantic on several SONEX flights in October 1997. They attributed the unusually low concentrations to transport from the marine tropical lower troposphere. Low O_3 values (below 20 ppbv) were also measured from the Falcon aircraft during POLINAT 2 [*Schumann et al.*, 2000, Figure 7]. Closer inspection of the data shows that the low O_3 values measured from the B-747 were all obtained in October as well. A similar feature is absent in the 1995 data where almost no values below 30 ppbv were observed.

To conclude, year-to-year differences in O_3 concentrations can be large because of the high sensitivity to the mean tropopause pressure, which in turn is controlled by the specific weather conditions in the given year. NO_x concentrations were similar in both years, both with respect to the geographical distribution and the frequency distribution, suggesting a high degree of representativity of the NOXAR NO_x measurements for a given season when a large domain such as the North Atlantic flight corridor is considered.

4.4. Ozone in a Potential Vorticity - Potential Temperature Frame of Reference

The dynamical properties of an air mass in the lower stratosphere can be characterized by its potential vor-

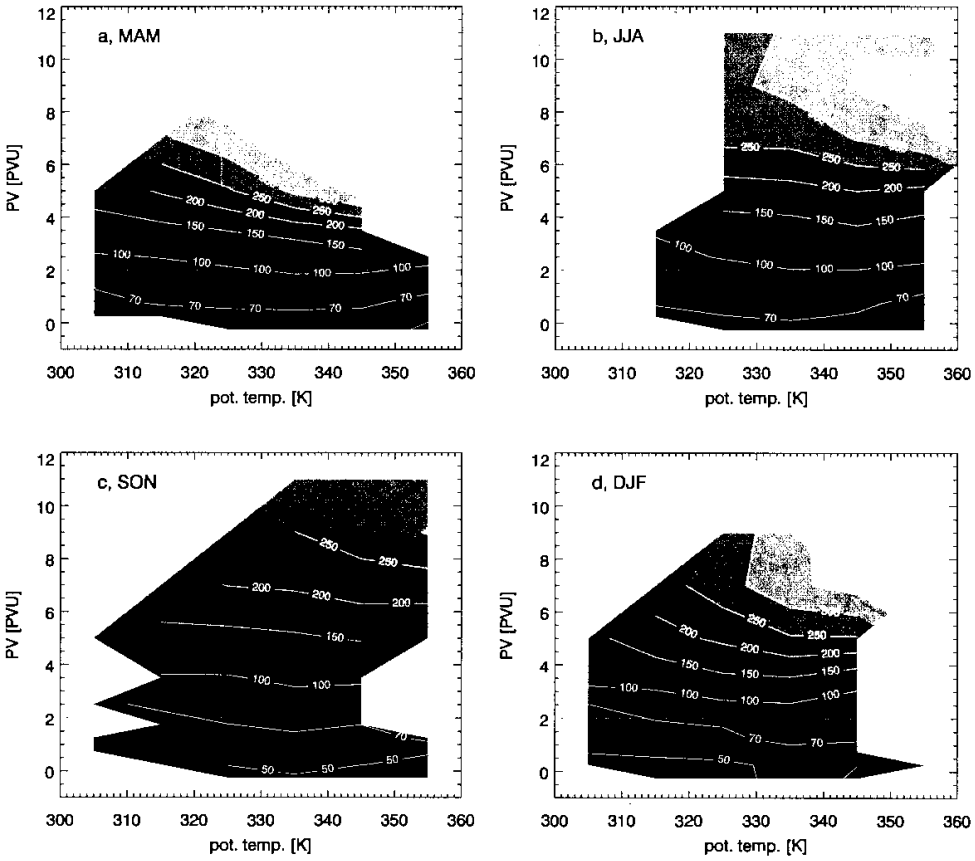

Figure 11. O_3 in a PV-θ frame of reference in the four seasons. Contours at 50, 70, 100, 150, 200, 250, 300, 350, 400, and 450 ppbv.

ticity (PV) and potential temperature (θ) [*Hoskins et al.* 1985]. In the absence of strong diabatic heating or cooling, these quantities are approximately conserved and air masses are therefore constrained to follow a line formed by the intersection of the surfaces of constant PV and θ. Air parcels with identical PV and θ are therefore closely connected and are expected to exhibit similar tracer concentrations. *Morgenstern and Marenco* [2000] analyzed four winters of MOZAIC O_3 measurements in an equivalent latitude (λ_e) - θ frame of reference. Equivalent latitudes were derived from analyzed potential vorticity fields and interpolated to the flight tracks. Potential vorticity is not well conserved in the troposphere and is therefore less suited to describe the properties of a tropospheric air mass. *Zahn et al.* [1999] found that in the troposphere deviations of potential temperature from monthly mean values at a given latitude and pressure level contains valuable information about the meridional displacement of an air mass from its original, or as they call it, "representative" latitude. In this section we simply analyze the measured O_3 concentrations as a function of PV and θ, being equivalent to the approach by *Morgenstern and Marenco* [2000]. Both *Morgenstern and Marenco* [2000] and *Zahn et al.* [1999] found that the large variability in tracer concentrations observed in an ordinary latitude-altitude frame of reference was significantly reduced when viewed in their specific parameter space.

Figure 11 shows the O_3 concentrations as a function of PV and θ in the four seasons. The dynamical tropopause is indicated by the dashed line at 2 PVU. The four figures show a similar behavior, with the lowest concentrations in the troposphere below 2 PVU and the highest values in the upper right corner, at high PV and θ values. At low PV, O_3 is approximately independent of θ and thus a function of PV alone. However, the dependence on θ increases with increasing PV. For instance, a value of 6 PVU in spring corresponds to an O_3 concentration of less than 250 ppbv at 310 K but to more than 400 ppbv at 350 K.

Lower stratospheric O_3 exhibits a strong seasonal cycle as a result of the Brewer-Dobson circulation [*Brewer*, 1949; *Dobson*, 1956]. This circulation is strongest during winter when wave activity in midlatitudes is strongest [*Holton et al.*, 1995; *Rosenlof*, 1995; *Appenzeller et al.*, 1996]. Consequently, poleward and down-

ward transport of O_3 from its main stratospheric production regions at low latitudes is strongest to the winter hemisphere, resulting in a lower stratospheric maximum in late winter to early spring. At 8 PVU and 340 K, for instance, O_3 varies between 420 ppbv in spring and only 240 ppbv in autumn. A pronounced seasonal cycle is also observed at the (2 PVU) dynamical tropopause. This prevents the use of a single O_3 concentration to discriminate between tropospheric and stratospheric air, as described earlier.

The above analysis suggests that the O_3-PV analogy in the tropopause region is not a simple relationship. The dependence on season [*Beekmann et al.*, 1994] and on potential temperature have to be accounted for. Owing to the reduction in tracer variability, PV-θ or equivalent coordinates are more suitable for the comparison of stratospheric observations from different stations or between observations and models than an ordinary latitude/longitude versus altitude frame of reference [*Morgenstern and Marenco*, 2000].

4.5. Tropopause-Scaled Vertical Profiles

Although the data presented here were sampled in a limited altitude range between 8500 m and 11600 m, the relative distance to the tropopause varied considerably. Here we calculate quasi-vertical profiles of NO_x and O_3 as a function of the relative vertical distance to the tropopause. Flight levels high above the tropopause are typically associated with a low tropopause and vice versa. A low tropopause, on the other hand, is associated with advection from high latitudes and a high tropopause with advection from low latitudes. In this sense the profiles have to be considered as quasi-vertical since they are also influenced by the meridional distribution. Note that these profiles are not directly comparable to real vertical profiles obtained for instance from balloon soundings. As stated above, a PV-theta frame of reference would be more suitable for this type of comparison.

Here we only present a comparison between the vertical profiles of NO_x over eastern North America and over the North Atlantic as they revealed large differences in all seasons (Figures 12 and 13). The North American profiles exhibit the highest values well below the local tropopause, particularly during spring and summer. The exceptionally high spring values in the UT over North America have already been discussed in section 4.1. Very high mean/median concentrations

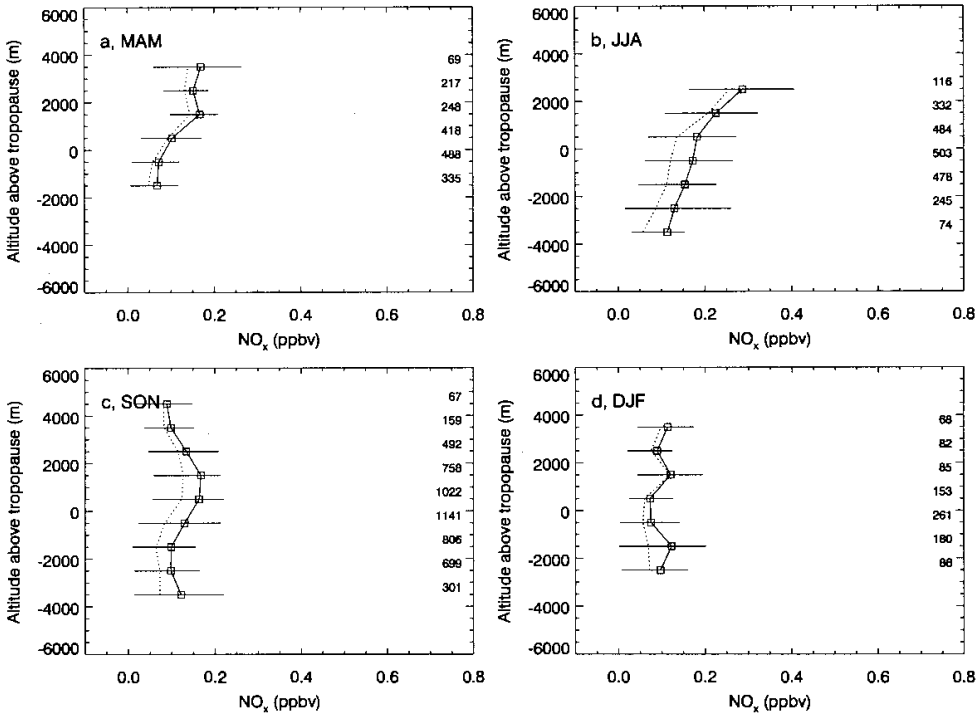

Figure 12. Tropopause-scaled vertical profiles of NO_x over the North Atlantic (40°-60°N, 10°-40°W) in the four seasons. The vertical coordinate is the altitude of the flight level relative to the dynamical tropopause (PV=2). Samples were grouped into bins of Δaltitude=1000 m centered at 500 m, 1500 m, etc. below and above the tropopause. Symbols are mean values of each bin. Horizontal bars represent the central 67% percentiles. Mean values are connected by solid lines, and median values are connected by dotted lines.

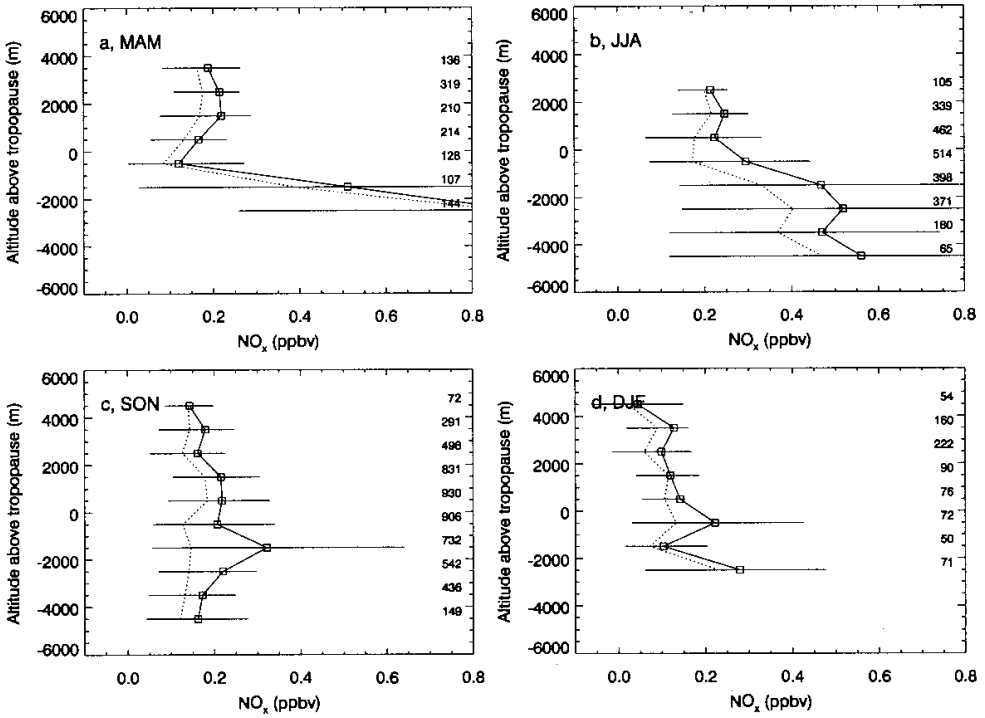

Figure 13. Same as Figure 12, but over North America (35°-60°N, 60°-100°W).

of about 0.5/0.4 ppbv are also observed at 2-4 km below the local tropopause in summer. The variability as indicated by the horizontal lines is strongly enhanced at these levels, and the mean values exceed the respective medians considerably. Mean concentrations above the tropopause are lower by 200-300 pptv than below the tropopause. Troposphere-to-stratosphere exchange over North America during summer may thus deliver significant amounts of NO_x to the lowermost stratosphere. A very different picture is obtained over the North Atlantic. Mean and median NO_x concentrations in summer steadily increase from about 110 pptv at 3-4 km below the tropopause to nearly 300 pptv at 2-3 km above the tropopause. The values at the highest stratospheric levels are comparable to those over North America, but in the UT the concentrations are lower by approximately a factor of 3 to 4 as compared to North America. The autumn profile over North America reveals a pronounced isolated maximum between 1 and 2 km below the tropopause. Mean upper tropospheric concentrations are about a factor of 2 higher than over the North Atlantic. Even the December profile is more perturbed in the the UT than over the North Atlantic. The UT over eastern North America appears to be strongly affected by local emission sources. Since these sources depend strongly on season, it is believed that convective upward transport of emissions from the surface and lightning activity are the largest contributors. Such a strong seasonality would not be expected if air traffic were the major source.

Tropopause scaled O_3 profiles at midlatitudes are shown in Figure 14. No distinction is made between continents and the North Atlantic because any differences are small. O_3 increases rapidly above the tropopause in all seasons. In spring the increase is the strongest and in autumn the weakest. Two kilometers above the tropopause the O_3 concentrations are approximately double as high in spring as in autumn, again showing the pronounced seasonal cycle caused by the Brewer-Dobson circulation. The vertical gradients decrease or even reverse at the highest relative altitudes. This clearly shows the difference between tropopause-scaled and real vertical O_3 profiles: Data points at high relative altitudes were sampled in situations with a very low tropopause indicating that the air was probably of polar origin. Despite the high altitude above the tropopause, such air masses were somewhat reduced in O_3, particularly in autumn. As expected, O_3 concentrations below the tropopause were highest in summer and lowest in winter and varied only little with altitude.

5. Summary and Conclusions

Insitu measurements of nitrogen oxides ($NO+NO_2$) and O_3 were performed from a passenger aircraft on a total of 623 flights between May 1995 and May 1996,

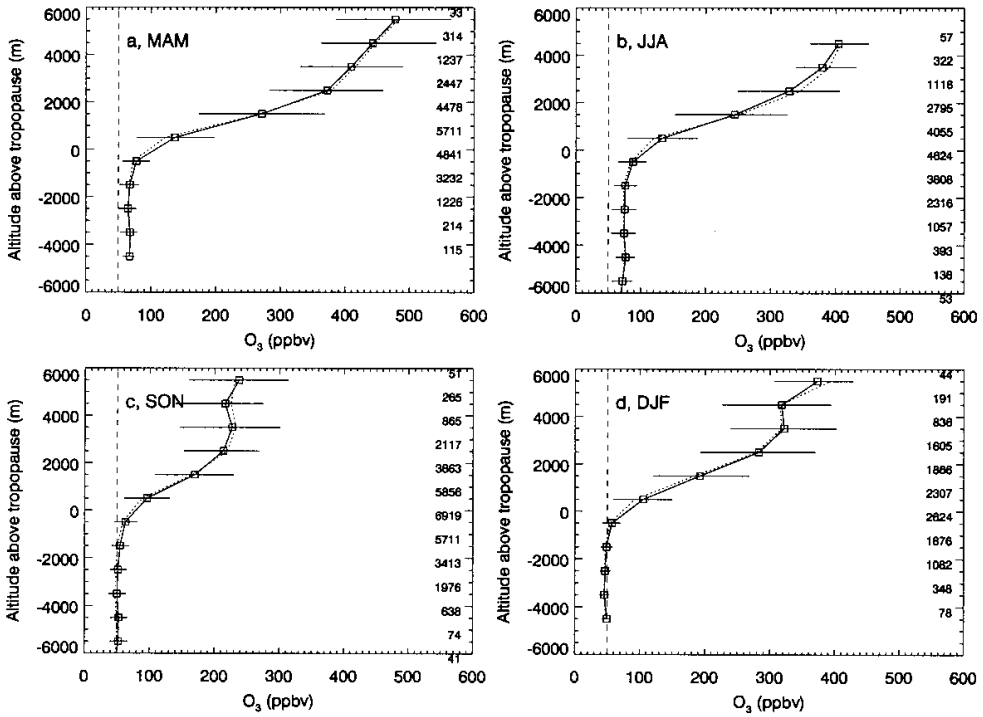

Figure 14. Tropopause-scaled vertical profiles of O_3 in midlatitudes (40°-60°N, 100°W-120°E) in the four seasons. For definition of symbols, see Figure 12. The dashed line represents a tropospheric reference concentration of 50 ppbv.

and between August and November 1997. The measurements constitute the most representative data set of NO_x concentrations available today for the UT and the LS and cover a large proportion of the northern hemisphere in all four seasons.

The NO_x observations at cruising altitudes (8.5 to 11.6 km) show the following prominent features:

1. A strong seasonal cycle exists in midlatitudes with a maximum in summer and a minimum in winter, both above and below the tropopause. In the LS, seasonal mean/median values are approximately 91/68 pptv in winter and 249/214 pptv in summer and show only a minor dependence on longitude. In the UT, however, strong differences are found between samples obtained over the continents and over the North Atlantic: Mean/median concentrations over eastern North America, for instance, are 230/122 pptv in winter and 407/278 pptv in summer. Over the North Atlantic the respective numbers are 93/61 pptv and 154/109 pptv.

2. A maximum over eastern North America exists in all seasons and is most pronounced during summer and spring. In these seasons, mean concentrations are 3 to 4 times higher than over the eastern North Atlantic. As demonstrated in two previous studies, this feature is closely related to the frequent occurrence of large-scale nitrogen oxide plumes in the UT downstream of convective and frontal systems [*Brunner et al.*, 1998; *Jeker et al.*, 2000]. Lightning activity and upward transport of NO_x from the surface thus appear to dominate the regional upper tropospheric NO_x budget.

3. A broad maximum extending from Europe to Siberia is observed during summer. Different from the U.S. maximum, this is mainly a summertime phenomenon. Over the North Atlantic, NO_x concentrations are generally lower in the UT than in the LS, except for winter. Over the continents, however, upper tropospheric NO_x can locally exceed the lower stratospheric values, in particular over North America during summer and spring.

4. There is a distinctly different seasonal behavior between Bombay and Hong Kong, with highest concentrations in spring and autumn, and lowest in summer and winter. The Asian summer Monsoon appears to produce a marked minimum between June and July, more than 2 times lower than mean spring and autumn values.

5. Frequency distributions are approximately lognormal with a long tail toward high concentrations. They are generally broader in the UT than in the LS due to larger local sources and sinks. Mean concentrations often exceed the respective median by far, in particular over the continents during spring and summer.

The O_3 observations show the following prominent features:

1. Ozone concentrations at cruising altitude are highly variable in midlatitudes because of variations in the altitude of the tropopause associated with synoptic weather systems and planetary waves. Quasi-stationary Rossby waves dominate the seasonal mean distribution.

2. As a result of the Brewer-Dobson circulation, O_3 in the midlatitude lowermost stratosphere exhibits a strong seasonal cycle: At a given value of potential vorticity and potential temperature, O_3 concentrations are 1.5 to 2 times as high in late spring than in late autumn.

3. Upper tropospheric O_3 in northern midlatitudes shows a broad maximum between June and August, similar to observations in the free troposphere obtained from balloon soundings [*Logan,* 1999]. The maximum appears about 2 months later than in the LS, and is slightly more pronounced over the continents than over the North Atlantic. These are both indications for the important, and possibly dominant, role of tropospheric photochemistry in the UT.

4. A different seasonal behavior is found in the UT between Bombay and Hong Kong with a spring maximum and a winter minimum.

The distribution of NO_x concentrations between Europe and North America was compared for the period August 12 to November 23 for 2 different years (1995 and 1997). The geographical distribution was similar in the 2 years, and the frequency distributions were nearly identical. This suggests that the NOXAR observations provide a good approximation to climatological mean NO_x distributions in the UT and the LS. However, even with a hypothetical perfect temporal and spatial coverage the measurements from a single year could not be regarded as being representative in a climatological sense. The ECHAM3/CHEM model for instance shows a year-to-year variability in monthly averaged NO_x concentrations at a given location of more than 15% [*Sausen and Koehler,* 1994].

The NOXAR observations are a first step toward a climatology of upper tropospheric and lower stratospheric nitrogen oxide concentrations. The European MOZAIC project will provide extensive measurements of NO_y in the near future and will be a valuable extension to this study. Moreover, a future NOXAR study is planned which will hopefully extend the observations to the Southern Hemisphere and include more tracers. The present and future observations from civil airliners provide extensive measurements in the UT and the LS and are therefore highly suitable for the validation of chemistry transport models.

Acknowledgments. We would like to acknowledge Hans Tremmel (DLR) for providing a table of NO_2 photolysis rates, Michel Bourqui (ETH) for trajectory calculations, and Hans Richner and Huw Davies (ETH) for valuable scientific discussions. The careful reading and suggestions from two reviewers are much appreciated. NOXAR was funded by the Swiss Federal Civil Aviation Authority (BAZL). We are grateful to Swissair for the generous support of the project and to ECO Physics Inc. (Switzerland) for the design of the instrumentation and support during operation. POLINAT 2 was funded by the European Commission (DG XII-D) (contract ENV4-CT95-043).

References

Appenzeller, C., J.R. Holton, and K.H. Rosenlof, Seasonal variation of mass transport across the tropopause, *J. Geophys. Res., 101,* 15,071-15,078, 1996.

Arnold, F., J. Schneider, K. Gollinger, H. Schlager, P. Schulte, P.D. Whitefield, D.E. Hagen, and P. van Velthoven, Observation of upper tropospheric sulfur dioxide and acetone pollution: Potential implications for hydroxyl radical and aerosol formation, *Geophys. Res. Lett., 24,* 57-60, 1997.

Atkinson, R., D.L. Baulch, R.A. Cox, R.F. Hamson Jr., J.A. Kerr, M.J. Rossi, and J. Troe, Summary of evaluated kinetic and photochemical data for atmospheric chemistry, IUPAC subcommittee on gas kinetic data evaluation for atmospheric chemistry, *J. Phys. Chem. Ref. Data, 26,* 521 pp., 1997.

Beekman, M., G. Ancellet, and G. Mégie, Climatology of tropospheric ozone in southern Europe and its relation to potential vorticity, *J. Geophys. Res., 99,* 12,841-12,853, 1994.

Berntsen, T.K., and I.S.A. Isaksen, Effects of lightning and convection on changes in tropospheric ozone due to NO_x emissions from aircraft, *Tellus, Ser. B, 51,* 766-788, 1999.

Bollinger, M. J., Chemiluminescent measurements of the oxides of nitrogen in the clean troposphere and atmospheric chemistry implications, Ph.D. thesis, 256 pp., Univ. of Colo., Boulder, 1982.

Bradshaw, J., D. Davis, G. Grodzinsky, S. Smyth, R. Newell, S. Sandholm, and S. Liu, Observed distributions of nitrogen oxides in the remote free troposphere from the NASA Global Tropospheric Experiment programs, *Rev. Geophys., 38,* 61-116, 2000.

Brasseur, G.P., R.A. Cox, D. Hauglustaine, I. Isaksen, J. Lelieveld, D.H. Lister, R. Sausen, U. Schumann, A. Wahner, and P. Wiesen, European scientific assessment of the effects of aircraft emissions, *Atmos. Environ., 32,* 2329-2418, 1998.

Brenninkmeijer, C.A.M., et al., CARIBIC - Civil aircraft for global measurement of trace gases and aerosols in the tropopause region, *J. Atmos. Oceanic Technol., 16,* 1373-1383, 1999.

Brewer, A.W., Evidence for a world circulation provided by the measurements of helium and water vapour distribution in the stratosphere, *Q. J. R. Meteorol. Soc., 75,* 357-363, 1949.

Brunner, D., One-year climatology of nitrogen oxides and ozone in the tropopause region, Ph.D. thesis, 181 pp., Swiss Fed. Inst. of Technol. (ETH), Zurich, Switzerland, 1998.

Brunner, D., J. Staehelin, and D. Jeker, Large-scale nitrogen oxide plumes in the tropopause region and implications for ozone, *Science, 282,* 1305-1309, 1998.

Cammas, J.-P., S. Jacoby-Koaly, K. Suhre, R. Rosset, aud A. Marenco, Atlantic subtropical potential vorticity barrier as seen by Measurements of Ozone by Airbus In-Service Aircraft (MOZAIC) flights, *J. Geophys. Res., 103,* 25,681-25,693, 1998.

Carroll, M.A., M. McFarland, B.A. Ridley, and D.L. Albritton, Ground-based nitric oxide measurements at Wallops Island, Virginia, *J. Geophys. Res., 90,* 12,853-12,860, 1985.

Carroll, M.A., D.D. Montzka, G. Hübler, K.K. Kelly, and G.L. Gregory, In situ measurements of NO_x in the Air-

borne Arctic Stratospheric Expedition, *Geophys. Res. Lett., 17,* 493-496, 1990.

Chalita, S., D.A. Hauglustaine, H. Le Treut, and J.-F. Müller, Radiative forcing due to increased tropospheric ozone concentrations, *Atmos. Environ., 30,* 1641-1646, 1996.

Crawford, J., et al., Photostationary state analysis of the NO_2-NO system based on airborne observations from the western and central North Pacific, *J. Geophys. Res., 101,* 2053-2072, 1996.

Crutzen, P.J., Tropospheric ozone: An overview, in *Tropospheric Ozone,* edited by I.S.A. Isaksen, pp. 3-32, D. Reidel, Norwell, Mass., 1988.

Dameris, M., V. Grewe, I. Köhler, R. Sausen, C. Brühl, J.-U. Grooß, and B. Steil, Impact of aircraft NO_x-emissions on tropospheric and stratospheric ozone, part II, 3-D model results, *Atmos. Environ., 32,* 3185-3200, 1998.

Danielsen, E.F., Stratospheric-tropospheric exchange based on radioactivity and potential vorticity, *J. Atmos. Sci., 25,* 25,502-25,518, 1968.

Davis, D.D., et al., A photostationary state analysis of the NO_2-NO system based on airborne observations from the subtropical/tropical North and South Atlantic, *J. Geophys. Res., 98,* 23,501-23,523, 1993.

Dentener, F., and P.J. Crutzen, Reaction of N_2O_5 on tropospheric aerosols: impact on the global distributions of NO_x, O_3, and OH, *J. Geophys. Res., 98,* 7149-7163, 1993.

Dias-Lalcaca, P., D. Brunner, W. Imfeld, W. Moser, and J. Staehelin, An automated system for the measurement of nitrogen oxides and ozone concentrations from a passenger aircraft - Instrumentation and first results of the NOXAR project, *Environ. Sci. Technol., 32,* 3228-3236, 1998.

Dobson, G.M.B., Origin and distribution of polyatomic molecules in the atmosphere, *Proc. R. Soc. Lond., Ser. A, 236,* 187-193, 1956.

Drummond, J.W., A. Volz, and D. H. Ehhalt, An optimized chemiluminescence detector for tropospheric NO measurements, *J. Atmos. Chem., 2,* 287-306, 1985.

Emmons, L.K., et al., Climatologies of NO_x and NO_y: A comparison of data and models, *Atmos. Environ., 31,* 1851-1904, 1997.

Emmons, L.K., D.A. Hauglustaine, J.-F. Müller, M.A. Carroll, G.P. Brasseur, D. Brunner, J. Staehelin, V. Thouret, and A. Marenco, Data composites of airborne observations of tropospheric ozone and its precursors, *J. Geophys. Res., 105,* 20,497-20,538, 2000.

Fabian, P., and P.G. Pruchniewicz, Meridional distribution of ozone in the troposphere and its seasonal variations. *J. Geophys. Res., 82,* 2063-2073, 1977.

Fishman, J., and P. Crutzen, The origin of ozone in the troposphere, *Nature, 274,* 855-858, 1978.

Fontijn, A., A.J. Sabadell, and R.J. Ronco, Homogeneous chemiluminescent measurement of nitric oxide with ozone, *Anal. Chem., 42,* 575-579, 1970.

Gao, R.S., et al., Partitioning of the reactive nitrogen reservoir in the lower stratosphere of the southern hemisphere: Observations and modeling, *J. Geophys. Res., 102,* 3935-3949, 1997.

Gardner, R.M (Ed.), ANCAT/EC global aircraft emissions inventories for 1991/92 and 2015, Report by the ECAC/ANCAT and EC working group, *EUR 18179,* 84 pp., Eur. Comm. Dir. - Gen. XI, Brussels, 1998.

Gettelman, A., The evolution of aircraft emissions in the stratosphere, *Geophys. Res. Lett., 25,* 2129-2132, 1998.

Gettelman, A., and S.L. Baughcum, Direct deposition of subsonic aircraft emissions into the stratosphere, *J. Geophys. Res., 104,* 8317-8327, 1999.

Grant, W.B., et al., A case study of transport of tropical marine boundary layer and lower tropospheric air masses to the norther midlatitude upper troposphere, *J. Geophys. Res., 105,* 3757-3770, 2000.

Grewe, V., and M. Dameris, Calculating the global mass exchange between stratosphere and troposphere, *Ann. Geophys., 14,* 431-442, 1996.

Grewe, V., M. Dameris, R. Hein, I. Köhler, and R. Sausen, Impact of future subsonic aircraft NO_x emissions on the atmospheric composition, *Geophys. Res. Lett., 26,* 47-50, 1999.

Grewe, V., D. Brunner, M. Dameris, J.L. Grenfell, R. Hein, D. Shindell, and J. Staehelin, Origin and variability of upper tropospheric nitrogen oxides and ozone at northern mid-latitudes, *Atmos. Environ., 35,* 3421-3433, 2001.

Hoerling, M.P., T.K. Schaack, and A.J. Lenzen, Global objective tropopause analysis, *Mon. Weather Rev., 119,* 1816-1831, 1991.

Hoinka, K.P., Statistics of the global tropopause pressure, *Mon. Weather Rev., 26,* 3303-3325, 1998.

Hoinka, K.P., M.E. Reinhardt, and W. Metz, North Atlantic air traffic withiu the lower stratosphere: Cruising times and corresponding emissions, *J. Geophys. Res., 98,* 23,113-23,131, 1993.

Holton, J.R., *An Introduction to Dynamical Meteorology,* 3^{rd} ed., 511 pp., Academic, San Diego, Calif., 1992.

Holton, J.R., P.H. Haynes, M.E. McIntyre, A.R. Douglass, R.B. Rood, and L. Pfister, Stratosphere-troposphere exchange, *Rev. Geophys., 33,* 403-439, 1995.

Hoskins, B., M. McIntyre, and W. Robertson, On the use and significance of isentropic potential vorticity maps, *Q. J. R. Meteorol. Soc., 111,* 877-946, 1985.

Hov, Ø., and F. Flatøy, Convective redistribution of ozone and oxides of nitrogen in the troposphere over Europe in summer and fall, *J. Atmos. Chem., 28,* 319-337, 1997.

Hurrell, J. W., Decadal trends in the North Atlantic Oscillation: Regional temperatures and precipitation, *Science, 269,* 676-679, 1995.

Intergovernmental Panel on Climate Change (IPCC), *Climate Change 1994: Radiative Forcing of Climate Change and an Evaluation of the IPCC IS92 Emission Scenarios,* edited by J.T. Houghton et al., 339 pp., Cambridge Univ. Press, New York, 1995.

Intergovernmental Panel on Climate Change (IPCC), *Aviation and the Global Atmosphere,* edited by J.E. Penner, Cambridge Univ. Press, New York, 1999.

Jacob, D.J., J.A. Logan, G.M. Gardner, R.M. Yewich, C.M. Spivakovsky, S.C. Wofsy, J.M. Munger, S. Sillman, and M.J. Prather, Factors regulating ozone over the United States and its export to the global atmosphere, *J. Geophys. Res., 98,* 14,817-14,826, 1993.

Jaeglé, L., D.J. Jacob, Y. Wang, A.J. Weinheimer, B.A. Ridley, T.L. Campos, G.W. Sachse, and D.E. Hagen, Sources and chemistry of NO_x in the upper troposphere over the United States, *Geophys. Res. Lett., 25,* 1709-1712, 1998.

Jeker, D., J. Staehelin, and D. Brunner, Nitrogen oxides and ozone from B-747 measurements (August to November 1997), in *POLINAT 2,* edited by U. Schumann, *EUR 18877 EN,* pp. 31-53, Eur. Comm., Luxembourg, 1999.

Jeker, D. P., L. Pfister, A. M. Thompson, D. Brunner, D.J. Boccippio, K.E. Pickering, H. Wernli, Y. Kondo, and J. Staehelin, Measurements of nitrogen oxides at the tropopause: Attribution to convection and correlation with lightning, *J. Geophys. Res., 105,* 3679-3700, 2000.

Jobson, B.T., S.A. McKeen, D.D. Parrish, F.C. Fehsenfeld, D.R. Blake, A.H. Goldstein, S.M. Schauffler, and J.W. Elkins, Trace gas mixing ratio variability versus lifetime in the troposphere and stratosphere: Observations, *J. Geophys. Res., 104,* 16,091-16,113, 1999.

Kawa, S.R., et al., Interpretation of NO_x/NO_y observations

from AASE-II using a model of chemistry along trajectories, *Geophys. Res. Lett., 20,* 2507-2510, 1993.

Kley, D., and M. McFarland, Chemiluminescence Detector for NO and NO_2, *Atmos. Technol., 12,* 63-69, 1980.

Kulshreshta, U.C., M. Jain, and D.C. Parashar, Concentrations and behavior of surface O_3, NO and NO_2 at Dehli, *Indian J. Radio Space Phys., 26,* 82-84, 1997.

Lacis, A.A., D.J. Wuebbles, and J.A. Logan, Radiative forcing of climate by changes in the vertical distribution of ozone, *J. Geophys. Res., 95,* 9971-9981, 1990.

Lamarque, J.-F., G.P. Brasseur, P.G. Hess, and J.-F. Müller, Three-dimensional study of the relative contributions of the different nitrogen sources in the troposphere, *J. Geophys. Res., 101,* 22,955-22,968, 1996.

Lelieveld, J., and P.J. Crutzen, Role of deep cloud convection in the ozone budget of the troposphere, *Science, 264,* 1759-1761, 1994.

Lippmann, M., Health effects of tropospheric ozone, *Environ. Sci. Technol., 25,* 1954-1962, 1991.

Liu, S. C., M. Trainer, F. C. Fehsenfeld, D. D. Parrish, E. J. William, D. W. Fahey, G. Hübler, and P. C. Murphy, Ozone production in the rural troposphere and implications for regional and global ozone production, *J. Geophys. Res., 92,* 4191-4207, 1987.

Logan, J.A., Tropospheric chemistry: A global perspective, *J. Geophys. Res., 86,* 7210-7254, 1981.

Logan, J.A., Tropospheric ozone: Seasonal behavior, trends, and anthropogenic iufluence, *J. Geophys. Res., 90,* 10,463-10,482, 1985.

Logan, J.A., An analysis of ozonesonde data for the troposphere: Recommendations for testing 3-D models and development of a gridded climatology for tropospheric ozone, *J. Geophys. Res., 104,* 16,115-16,149, 1999.

Marenco, A., et al., Measurement of ozone and water vapor by Airbus in-service aircraft: The MOZAIC airborne program, An overview, *J. Geophys. Res., 103,* 25,631-25,642, 1998.

Matsueda, H., and H.Y. Inoue, Measurements of atmospheric CO_2 and CH_4 using a commercial airliner from 1993 to 1994, *Atmos. Environ., 30,* 1647-1655, 1996.

Morgenstern, O., and A. Marenco, Wintertime climatology of MOZAIC ozone based on the potential vorticity and ozone analogy, *J. Geophys. Res., 105,* 15,481-15,493, 2000.

Naja, M., and S. Lal, Changes in surface ozone amount and its diurnal and seasonal patterns, from 1954-55 to 1991-93, measured at Ahmedabad (23N), India, *Geophys. Res. Lett., 23,* 81-84, 1996.

NASA, The atmospheric effects of subsonic aircraft, *NASA Ref. Publ., 1400,* 143 pp., 1997.

Nastrom, G.D., Ozone in the upper troposphere from GASP measurements, *J. Geophys. Res., 84,* 3683-3688, 1979.

Pickering, K.E., Y. Wang, T. Wei-Kuo, C. Price, and J.-F. Müeller, Vertical distributions of lightning NO_x for use in regional and global chemical transport models, *J. Geophys. Res., 103,* 31,203-31,216, 1998.

Price, C., and D. Rind, A simple lightning parameterization for calculating global lightning distributions, *J. Geophys. Res., 97,* 9919-9933, 1992.

Prinz, B., Ozone effects on vegetation, in *Proceedings of the NATO Advanced Workshop on Regional and Global Ozone Interaction and Its Environmental Consequences,* edited by I.S.A. Isaksen, pp. 161-184, D. Reidel, Norwell, Mass., 1988.

Ravetta, F., G. Ancellet, J. Kowol-Santen, R. Wilson, and D. Nedeljkovic, Ozone, temperature, and wind field measurements in a tropopause fold: Comparison with a mesoscale model simulation, *Mon. Weather Rev., 127,* 2641-2653, 1999.

Ridley, B.A., M.A. Carroll, and G.L. Gregory, Measurements of nitric oxide in the boundary layer and free troposphere over the Pacific Ocean, *J. Geophys. Res., 92,* 2025-2047, 1987.

Ridley, B.A., S. Madronich, R.B. Chatfield, R.B. Walega, and R.E. Shetter, Measurements and model simulations of the photostationary state during the Mauna Loa Observatory Photochemistry Experiment: Implications for radical concentrations and ozone production and loss rates, *J. Geophys. Res., 97,* 10,375-10,388, 1992.

Roelofs, G.-J., J. Lelieveld, and R. van Dorland, A three-dimensional chemistry/general circulation model simulation of anthropogenically derived ozone in the troposphere and its radiative climate forcing, *J. Geophys. Res., 102,* 23,389-23,401, 1997.

Rosenlof, K.H., Seasonal cycle of the residual mean meridional circulation in the stratosphere, *J. Geophys. Res., 100,* 5173-5191, 1995.

Ruggaber, A., R. Dlugi, and T. Nakajima, Modelling of radiation quantities and photolysis frequencies in the troposphere, *J. Atmos. Chem., 18,* 171-210, 1994.

Sausen, R., and I. Köhler, Simulating the global transport of nitrogen oxides emissions from aircraft, *Ann. Geophys., 12,* 394-402, 1994.

Schiff, H.I., D. Pepper, and B.A. Ridley, Tropospheric NO measurements up to 7 km, *J. Geophys. Res., 84,* 7895-7897, 1979.

Schlager, H., P. Konopka, P. Schulte, U. Schumann, H. Ziereis, F. Arnold, M. Klemm, D.E. Hagen, P.D. Whitefield, and J. Ovarlez, In situ observations of air traffic emission signatures in the North Atlantic flight corridor, *J. Geophys. Res., 102,* 10,739-10,750, 1997.

Schumann, U., On the effect of emissions from aircraft engines on the state of the atmosphere, *Ann. Geophys., 12,* 365-384, 1994.

Schumann, U. (Ed.), Pollution from aircraft emissions in the North Atlantic flight corridor (POLINAT), *Air Pollut. Res. Rep. 58, Publ. EUR 16978 EN,* 303 pp., Off. for Off. Publ. of the Eur. Communities, Luxemburg, 1996.

Schumann, U., H. Schlager, F. Arnold, R. Baumann, O. Haschberger, and O. Klemm, Dilution of aircraft exhaust plumes at cruise altitudes, *Atmos. Environ., 32,* 3097-3104, 1998.

Schumann, U., H. Schlager, F. Arnold, J. Ovarlez, H. Kelder, Ø. Hov, G. Hayman, I.S.A. Isaksen, J. Staehelin, and P.D. Whitefield, Pollution from aircraft emissions in the North Atlantic flight corridor: Overview on the POLINAT projects, *J. Geophys. Res., 105,* 3605-3631, 2000.

Seiler, W., and C. Junge, Carbon monoxide in the atmosphere, *J. Geophys. Res., 75,* 2217-2226, 1970.

Seinfeld, J.H., and S.N. Pandis, *Atmospheric Chemistry and Physics,* 1326 pp., John Wiley, New York, 1998.

Stohl, A., and T. Trickl, A textbook example of long-range transport: Simultaneous observation of ozone maxima of stratospheric and North American origin in the free troposphere over Europe, *J. Geophys. Res., 104,* 30,445-30,462, 1999.

Thakur, A.N., H.B. Singh, P. Mariani, Y. Chen, Y. Wang, D.J. Jacob, G. Brasseur, J.-F. Müller, and M. Lawrence, Distribution of reactive nitrogen species in the remote free troposphere: Data and model comparisons, *Atmos. Environ., 33,* 1403-1422, 1999.

Thompson, A. M., H. B. Singh, and H. Schlager, Subsonic Assessment Ozone and Nitrogen Oxide Experiment (SONEX) and Pollution From Aircraft Emissions in the North Atlantic Flight Corridor (POLINAT 2), *J. Geophys. Res., 105,* 3595-3603, 2000.

Thouret, V., A. Marenco, P. Nédélec, and C. Grouhel,

Ozone climatologies at 9-12 km altitude as seen by the MOZAIC airborne program between September 1994 and August 1996, *J. Geophys. Res., 103,* 25,653-25,679, 1998.

Wirth, V., Thermal versus dynamical tropopause in upper-tropospheric balanced flow anomalies, *Q. J. R. Meteorol. Soc., 126,* 299-317, 2000.

World Meteorological Organisation (WMO), Scientific assessment of ozone depletion: 1998, Rep. 44, Geneva, Switzerland.

Zachariasse, M., P.F.J. van Velthoven, H.G.J. Smit, J. Lelieveld, T.K. Mandal, and H. Kelder, Influence of stratosphere-troposphere exchange on tropospheric ozone over the tropical Indian Ocean during the winter monsoon, *J. Geophys. Res., 105,* 15,403-15,416, 2000.

Zahn, A., R. Neubert, M. Maiss, and U. Platt, Fate of long-lived trace species near the Northern Hemispheric tropopause: Carbon dioxide, methane, ozone, and sulfur hexafluoride, *J. Geophys. Res., 104,* 13,923-13,942, 1999.

D. Brunner, J. Staehelin, D. Jeker, and H. Wernli, Institute for Atmospheric and Climate Science, Swiss Federal Institute of Technology, ETH Hönggerberg HPP, 8093 Zurich, Switzerland. (brunner@atmos.umnw.ethz.ch; staehelin@atmos.umnw.ethz.ch; jeker@atmos.umnw.ethz.ch; wernli@atmos.umnw.ethz.ch)

U. Schumann, Institut für Physik der Atmosphäre, DLR, Oberpfaffenhofen, Postfach 1116, 82230 Wessling, Germany. (Ulrich.Schumann@dlr.de)

(Received September 12, 2000; revised December 16, 2000; accepted May 14, 2001 .)